The Molecular Mechanisms Underlying the Cytochrome C Oxidase Dysfunction-Induced Accelerated Apoptosis

Inaugural-Dissertation

Zur

Erlangung des Doktorgrades

der Mathematisch-Naturwissenschaftlichen Fakultät

der Universität zu Köln

vorgelegt von

Stephan Schüll

aus Hilden

Berichterstatter: Prof. Dr. Elena Rugarli

Prof. Dr. Rudolf Wiesner

Tag der mündlichen Prüfung: 21.05.2014

TABLE OF CONTENTS

Abbreviations

(Frequently used terms only)

AD	Alzheimer's disease
aSMase	acid Sphingomyelinase
3-NP	3-Nitropropionic acid
Bak	Bcl-2 antagonist killer 1
Bax	Bcl-2 associated x protein
Bcl-2	B-cell lymphoma 2
Bcl-xL	B-cell lymphoma extra-large
BH	Bcl-2 homology
Bid	BH3-interacting domain death antagonist
BSA	Bovine serum albumin
CerS	Ceramide synthase
CL	Cardiolipin
COX	Cytochrome c oxidase
Cybrid	Cellular hybrid
e^-	Electron
ER	Endoplasmic reticulum
H	hours
H_2O_2	Hydrogen peroxide
IMM	Inner mitochondrial membrane
kDa	Kilodalton
DMSO	Dimethyl sulfoxide
DKO	Double knockout
DTT	Dithiothreitol

EDTA	Ethylenediaminetetraacetic acid
FB1	Fumonisin B1
IMS	Intermembrane space
IF	Immunofluorescence
IP	Immunoprecipitation
M (p/n/µ/m)	Molar; pico-, nano-, mikro-, milli-
MOMP	Mitochondrial outer membrane permeabilization
mtDNA	mitochondrial DNA
nDNA	nuclear DNA
nSMase	neutral Sphingomyelinase
OMM	Outer mitochondrial membrane
ON	Over night
OXPHOS	Oxidative phosphorylation
O_2^-	Superoxide anion
PAGE	Polyacrylamide gel electrophoresis
PBS	Phosphate buffered saline
PCR	Polymerase chain reaction
PD	Parkinson's disease
ROS	Reactive oxygen species
RC	Respiratory chain
RT	Room temperature
SDS	Sodium dodecyl sulfate
SEM	Standard error of the mean
STS	Staurosporine
WB	Western blot

Abstract

Apoptosis, the physiological cell death, is an essential component of cellular homeostasis and tissue regeneration, and the dysregulation of apoptosis culminates in multiple human diseases. Whereas the failure to execute timely programmed cell death in renovating tissues contributes to cancer, excessive apoptosis in post-mitotic tissues precipitates degenerative states, aging and aging-associated diseases.

Research work within the last two decades has shown that tissue degeneration caused by mitochondrial oxidative phosphorylation (OXPHOS) defects is associated with excessive apoptosis. However, it is unclear how OXPHOS-dysfunctions interfere with the apoptotic machinery and how this impacts on tissue degeneration.

In this context we demonstrate that solely the chemical induction of cytochrome c oxidase (COX) deficiency, which is among the most common defects found in mitochondrial diseases, exclusively and dramatically increases the Bcl-2 dependent apoptotic response towards oxidative stress. Furthermore, we could widen and reconfirm our findings in COX-deficient cybrids harboring an mtDNA-encoded deletion of COX subunit I as well as in murine fibroblast devoid of COX-assembly factor COX10. These findings indicate a general mechanism of COX-deficiency induced apoptosis by oxidative stress. Moreover, our data highlight that COX-deficiency is accompanied by an increased *de novo* synthesis and accumulation of the sphingolipid species ceramide. Due to their chemical properties especially ceramides with an acyl side-chain length of $C_{16:0}$ have conclusively and repeatedly been demonstrated to induce apoptosis by pore-formation and by contributing to pro-apoptotic Bax and Bak induced permeabilization of the mitochondrial outer membrane (MOMP). Correspondingly, we show that the inhibition of endoplasmic reticulum-resident specific ceramide synthases abrogates enhanced apoptosis induced by mitochondrial respiratory chain-dysfunction. In particular, we identify ceramide synthase 6 (CerS6) as the key mediator of $C_{16:0}$ ceramide induced apoptosis to oxidative stress: While down-regulation of CerS6 protects COX-deficient cells from oxidative stress, overexpression of CerS6 introduces susceptibility towards oxidative stress in COX-functional cells.

In summary, our findings identify ceramide accumulation and in particular CerS6 as important components of the apoptotic response of COX-deficient cells towards oxidative stress and provide new insights into how mitochondrial dysfunction interferes with the apoptotic machinery and may impact on tissue homeostasis.

Zusammenfassung

Apoptose, besser bekannt als physiologischer Zelltod, ist ein wichtiger Bestandteil der Zell-Homöostase sowie der Geweberegeneration. Ein Ungleichgewicht im physiologischen Zelltod kann die Entstehung multipler Krankheiten beim Menschen begünstigen. So ist beispielsweise eine verminderte oder gänzlich reduzierte Apoptose ursächlich für die Entstehung von Krebs, wohingegen exzessive und deregulierte Apoptose in postmitotischen Gewebe zu degenerativen Krankheiten bzw. altersbedingten Krankheitserscheinungen führen kann.
Die Forschungsarbeit der letzten zwei Jahrzehnte hat aufgezeigt, dass die Gewebedegeneration aufgrund defekter mitochondrialer oxidativer Phosphorylierung (OXPHOS) mit erhöhter Apoptose assoziiert ist. Hierbei ist jedoch unklar, wie genau sich Störungen der OXPHOS auf den Wirkungsmechanismus der Apoptose auswirken und wie dies dann zur Gewebedegeneration beiträgt.

In diesem Zusammenhang können wir zeigen, dass ausschließlich der durch chemische Inhibition hervorgerufene Defekt der Cytochrome C Oxidase (COX), eine der am häufigsten auftretenden Defekte bei mitochondrialen Erkrankungen, ursächlich für eine erhöhte Bcl-2 abhängige Apoptose aufgrund von oxidativem Stress ist. Diese Befunde konnten durch weitere Untersuchungen in einer COX-defizienten Cybridlinie, welche einen mitochondrial-kodierten Defekt der strukturellen COX-Untereinheit I enthält, sowie in murinen Knockout-Fibroblasten des Assembly-Faktors COX10 bestätigt und untermauert werden. Unsere Untersuchungen deuten daher auf einen generellen Wirkungsmechanismus der durch COX-Defizienz induzierten Apoptose nach oxidativem Stress hin.

Des Weiteren belegen unsere Untersuchungen, dass Defekte der COX mit einer erhöhten *de novo* Synthese und der Anhäufung von Ceramiden einhergehen. Für Ceramide, insbesondere solcher mit einer $C_{16:0}$ Seitenkette, konnte in der Vergangenheit wiederholt gezeigt werden, dass sie bei der Permeabilisierung der äußeren mitochondrialen Membran (engl. MOMP) mittels der pro-apoptotischen Proteine Bax und Bak eine wichtige Funktion als Porenbildner einnehmen. In diesem Zusammenhang zeigt die hier vorliegende Arbeit, dass die durch oxidativen Stress hervorgerufene Apoptose in COX-defizienten Zellen durch die Blockade der sich am endoplasmatischen Retikulum befindenden Ceramide-Synthasen vollständig aufgehoben werden kann. Insbesondere können wir hierbei zeigen, dass die Ceramide-Synthase 6 (CerS6) eine Schlüsselrolle in der Apoptose von COX-defizienten Zellen auf oxidativen Stress einnimmt:

Während eine Verminderung der CerS6-Expression in COX-defizienten Zellen vor oxidativem Stress schützt, bewirkt die Überexpression von der CerS6, dass normal respirierende Zellen ohne COX-Defekt gegenüber oxidativem Stress anfällig werden.

Zusammenfassend zeigt die vorliegende Arbeit, dass die Akkumulation von Ceramiden sowie die CerS6 essentielle Bestandteile der durch oxidativen Stress-induzierten Apoptose in Zellen mit defekter COX sind. Unsere Arbeit ermöglicht neue Einblicke in die Auswirkungen von mitochondrialen Defekten auf den Prozess des physiologischen Zelltods und wie sich dies auf die Gewebe-Homöostase auswirken könnte.

Introduction

Apoptosis, the controlled demolition of a cell

The indispensable physiological process of programmed cell death was first described by Kerr, Wyllie and Currie around forty years ago (Kerr et al., 1972). Based on its characteristic morphological changes including chromatin condensation, fragmentation of the nucleus, organelle degradation as well as cell shrinkage and blebbing it was termed apoptosis, referring to the Greek term for "dropping off" petals from flowers (Williams et al., 1974; Wyllie et al., 1980). The result of these morphological changes is the formation of cellular fragments termed apoptotic bodies which are finally cleared by phagocytes, preventing damage to the surrounding tissue by uncontrolled spilling of cellular debris and allowing the recovery of precious cellular constituents (Reddien et al., 2001; Ravichandran & Lorenz, 2007). These processes are mainly, but not exclusively, orchestrated by members of a family of cysteine proteases known as caspases. Caspases cleave their substrates after specific aspartate residues (the "asp" in the word caspase), while the hydrolysis of the peptide bond is catalyzed by a cysteine in the active site (the "c" in the word caspase) (Yuan et al., 1993; Nicholson & Thornberry, 1997). The activation of caspases occurs via two major pathways, referred to as extrinsic and intrinsic pathway of apoptosis (Figure 1.1).

The extrinsic pathway of apoptosis is activated by the binding of extracellular death ligands of the *tumor necrosis factor* (TNF) family such as FAS-ligand, TNF-α or TRAIL to death receptors on the surface of the plasma membrane. Ligand-binding provokes receptor oligomerization and the recruitment of adapter proteins like *FAS associated death domain* (FADD), which in turn recruits the initiator caspase 8 to form the *death inducing signaling complex* (DISC) (Kischkel et al., 1995; Boatright et al., 2003). Caspase 8 becomes activated and then directly cleaves and activates the downstream executioner caspases 3 and 7 which conduct protein degradation and apoptosis.

The intrinsic pathway of apoptosis can be initiated cell-autonomously by overwhelming intracellular stress such as DNA damage, viral infection or growth factor withdrawal. Because intrinsic apoptosis arises from the *mitochondrial outer membrane permeabilization* (MOMP) followed by the release of pro-apoptotic *intermembrane space* (IMS) proteins like cytochrome c into the cytosol, it is also referred to as the mitochondrial pathway of apoptosis. The release of

cytochrome c into the cytosol stimulates the ATP-dependent oligomerization with *apoptotic protease activating factor 1* (APAF1) to form the apoptosome, which in turn catalyzes the auto-activation of initiator caspase 9 (Liu et al., 1996; Li et al., 1997). Activated caspase 9, like caspase 8, then directly cleaves and activates executioner caspases. Both pathways are interconnected by the capability of caspase 8 to proteolytically activate Bid, a BH3-only member of the Bcl-2 protein family, which upon truncation (then called tBid) translocates to mitochondria and initiates MOMP (Figure 1.1).

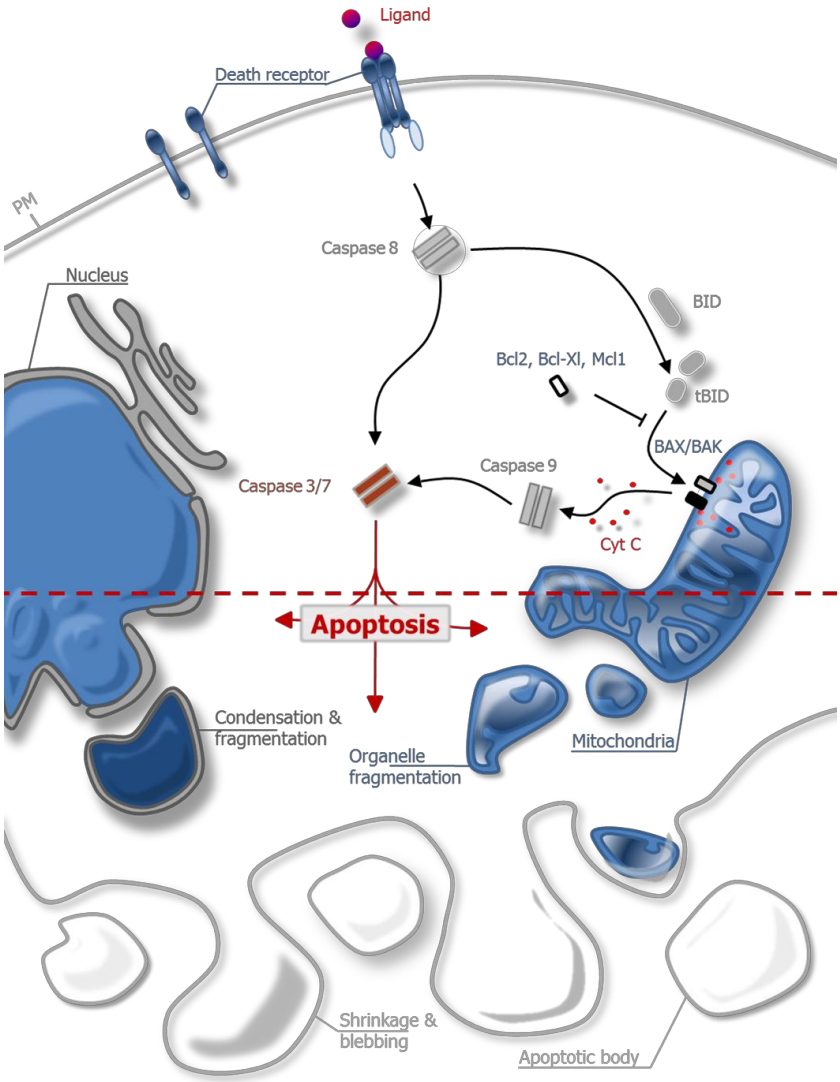

Figure 1.1 | Extrinsic and intrinsic pathway of apoptosis

Upon binding of a death ligand to its specific receptor on the surface of the plasma membrane, the DISC complex constitutes and initiator caspase 8 becomes activated. Caspase 8 either directly activates

executioner caspases 3/7 or indirectly by cleaving BH3-only protein Bid. tBid activates pro-apoptotic Bax/Bak on the outer mitochondrial membrane while activation of Bax/Bak is antagonized by anti-apoptotic Bcl-2 proteins. Bax/Bak induce MOMP, resulting in the release of IMS proteins like cytochrome c and activation of initiator caspase 9. In turn caspase 9 cleaves and activates caspase 3/7, thereby executing the apoptotic demise of the cell. PM, plasma membrane; Cyt c, cytochrome c.

Point of no return: Mitochondrial outer membrane permeabilization

MOMP is considered as the point of no return, making it profoundly important to provide well-balanced regulatory mechanisms which are carried out by proteins of the *B- cell lymphoma 2* (Bcl-2) family. Based on their role in conducting apoptosis, Bcl-2 proteins are subdivided into three classes: the class of pro-apoptotic Bcl-2 proteins like Bax and Bak which are responsible for MOMP, the class of anti-apoptotic Bcl-2 proteins such as Bcl-2, Bcl-xL and Mcl-1 which counteract MOMP by directly binding and inhibiting Bax or Bak, and the divergent class of BH3-only proteins including Bad, Bik, Bid, Bim, Bmf, Noxa and Puma that can bind and regulate the activity of pro- and anti-apoptotic Bcl-2 proteins likewise. Recent evidence suggests that BH3-only proteins de-repress and liberate Bax and Bak by direct binding and inhibition of anti-apoptotic family members (Westphal et al., 2014). By contrast, an opposing model postulates direct activation of Bax and Bak by BH3-only proteins including Bim, tBid and Puma (Tait & Green 2010).

The mitochondrial apoptotic pathway depends on the activation of Bax and Bak, either of which is sufficient to drive MOMP in the majority of cells. Upon cytotoxic stress, the hydrophobic BH3-domain of Bax and Bak becomes exposed and facilitates the generation of stable homo-oligomers that insert into the outer mitochondrial membrane, forms membrane pores and thereby provokes the release of pro-apoptotic IMS-proteins (Zha et al., 1996; Dewson et al., 2008; Kim et al., 2009). The insertion of Bax and Bak into the outer mitochondrial membrane represents a central prerequisite for their pro-apoptotic action which is directed by a C-terminal tail anchor (TA). The tail anchor potentiates the association of cellular proteins mainly with mitochondria or the *endoplasmic reticulum* (ER), where they are inserted into the lipid membrane via a single membrane span. Pro-apoptotic Bak resides as an inactive monomer in the outer mitochondrial membrane where it is constantly bound and inactivated by anti-apoptotic Mcl-1 and Bcl-xL (Willis et al. 2005). Unlike Bak and the majority of TA-proteins, including the anti-apoptotic Bcl-2 family members Bcl-2 and Bcl-xL that are constitutively bound

to their target membranes, Bax in its monomeric inactive state predominantly appears in the cytosol and translocates to the mitochondria upon activation (Hsu & Youle 1998). Whereas only a minor fraction of Bax has been shown to be loosely attached to the outer mitochondrial membrane, the solubility of Bax is effectively regulated by the reduced exposure of its hydrophobic C terminus (Suzuki et al., 2000). Recent data conclusively demonstrated that Bax exists in a dynamic equilibrium between the cytosolic and mitochondrial compartment and that the subcellular localization of Bax is constantly maintained by Bcl-xL (Schellenberg et al. 2013; Edlich et al. 2011).

Previous work revealed that the pore formation in the outer mitochondrial membrane is not only controlled by the expression status of Bcl-2 protein family members, but that in addition the lipid composition of the mitochondrial outer membrane is also critical for the action of Bcl-2 proteins. The vast majority of membrane phospholipids and lipid precursors are synthesized in the ER and are delivered via vesicle transport or *lipid-transfer proteins* (LTP) for further processing into the Golgi apparatus, peroxisomes and mitochondria (Lev 2012). Initial studies performed on unilamellar vesicles mimicking outer mitochondrial membranes provided conceptional advances concerning the interplay of Bcl-2 proteins and mitochondrial lipids. Further work has demonstrated that the embedment of pro-apoptotic Bax together with tBid (Lovell et al. 2008; Shamas-Din et al. 2013) as well as anti-apoptotic Bcl-xL (Billen et al., 2008) into membrane compartments mimicking the outer mitochondrial membrane is necessary for the regulation of Bax.

The inner and outer mitochondrial membranes are predominantly composed by the two phospholipids *phosphatidylcholine* (PC) and *phosphatidylethanolamine* (PE), representing approximately 70-80% of the total mitochondrial membrane lipid content. *Phosphatidylinositol* (PI) and the diglycerophospholipid *cardiolipin* (CL) account for 10-15%, while other phospholipids including sphingomyelins are only detectable in trace amounts (Horvath & Daum, 2013). CL is unique among the mitochondrial phospholipids in that it is mitochondria-exclusive and mainly resides in the inner mitochondrial membrane. Beside its function in membrane fluidity, supercomplex assembly and stability (Pfeiffer et al. 2003), CL has been demonstrated to be essential for tBid mediated Bax oligomerization and pore formation in liposomes (Lutter et al., 2000; Kuwana et al., 2002) and early oxidation of CL in apoptosis is critical for the dissociation of cytochrome c from the inner mitochondrial membrane and release into the cytosol (Kagan et al., 2005; Choi et al., 2007). Accordingly, overexpression of *phospholipid*

scramblase 3 (PLS3), a mitochondrial flippase responsible for the transfer of CL between inner and outer mitochondrial membrane compartments, increased CL exposure on the mitochondrial surface and enhanced mitochondrial apoptosis upon TNF-α treatment (Liu et al., 2008). Furthermore, perturbation of CL biosynthesis is sufficient to sensitize mitochondria to both extrinsic and intrinsic apoptotic stress (Potting et al. 2013).

In addition to CL, distinct sphingolipids species have been shown not only to be involved in membrane architecture, but also in numerous and diverse cellular processes such as proliferation, differentiation, senescence, inflammation as well as in the induction and inhibition of apoptosis (Hannun & Obeid 2008). In this regard, ceramides have become the center of attention since the early discoveries of the molecular principles of apoptosis (Obeid et al., 1993) and the pivotal function of ceramides in mediating apoptosis has been intensely described (Tirodkar & Voelkel-Johnson 2012; Chipuk et al. 2012). The vast majority of mammalian sphingolipids have a $C_{18:0}$ sphingoid base linked to a varying side chain, whereas the head group is either unmodified (ceramides), contains a phosphocholine group derived from phosphatidylcholine (sphingomyelins) or is linked to mono- or oligosaccharides (cerebrosides and gangliosides, respectively). Ceramides exert their physiological role in a fatty acyl side-chain specific manner. Here, especially ceramides containing a $C_{16:0}$ side chain have been shown to participate in Bax/Bak dependent MOMP by versatile stress stimuli including death ligand binding (Matsko et al., 2001), UV light (Kashkar et al., 2005) and irradiation (Lee et al. 2011), though the exact biochemical nature of the interplay between ceramides and Bcl-2 proteins in pore formation remains controversial (discussed in Renault & Chipuk, 2014).

Dysregulation of apoptosis

In order to maintain the cellular orchestra of constant renovation and demise, multicellular organisms are not only highly dependent on accurate regeneration and replacement of cells, but also on their controlled degradation. Therefore, the prerequisite of tissue homeostasis is that if cells are constantly renewed, an equal amount must necessarily die. Initial experiments in the model organism *Caenorhabditis elegans* illustrated the critical role of apoptosis in the embryogenesis and development of organisms (Ellis & Horvitz 1986). Similar observations in flies and vertebrates like zebrafish and rodents underscored the fundamental role of apoptosis in embryogenesis and development. For example, pro-apoptotic Bax and Bak were shown to be crucial for embryonic development in mice, given that the majority of double knockout animals

die prenatally or display multiple developmental defects (Lindsten et al. 2000). Additionally, the generation of caspase knockout mice further underlined the importance of effective apoptosis in embryogenesis and development, revealing prenatal mortality or neurological defects in adulthood in caspase 3, 8 and 9 knockout mice (reviewed in Kumar, 2007). In addition to its involvement in embryonic development, imbalanced apoptosis in adult tissues may cause defects in tissue homeostasis and prelude the progression of numerous different diseases. Accordingly, failure to precisely execute timely controlled cell death in renovating tissues contributes to the formation of cancer. On the other hand, excessive programmed cell death particularly in post-mitotic tissue is assumed to precipitate degenerative states and is implicated in the progression of aging and aging associated diseases like Alzheimer's disease and Parkinson.

Inhibition of Apoptosis and cancer

There is a general consensus that the transformation of healthy cells into tumorigenic and malignant cells is characterized by the acquisition of eight biological capabilities in a multistep process caused by genomic instabilities: 1.) Reprogramming of energy metabolism, 2.) escaping immune response, 3.) sustaining proliferative signaling and 4.) evading growth suppressors, 5.) inducing angiogenesis, 6.) activating invasion and metastasis, 7.) enabling replicative immortality and 8.) resisting cell death (Hanahan & Weinberg 2011). The importance of apoptosis and the implications of its alteration in the progression of different malignancies has accompanied the advances made in understanding the molecular mechanism, regulation and physiological role of apoptosis ever since (Evan & Littlewood 1998). Indeed, already in the initial work done by Kerr and coworkers, apoptosis was correlated to therapeutically induced tumor regression (Kerr et al. 1972). Accordingly, apoptosis reduction in cancer progression and maintenance can be associated with defective death receptor signaling, dysregulated caspase activation and misbalances in the interaction of pro- and anti-apoptotic Bcl-2 proteins. Here, overexpression of anti-apoptotic Bcl-2 proteins like Bcl-2, Mcl1 and Bcl-xL and transcriptional and/or post-transcriptional repression of pro-apoptotic Bcl-2 members like Bax and Bak and BH3-only proteins have been demonstrated as iterant traits of cancer cells (Beroukhim et al. 2010; Kelly & Strasser 2011). On the basis of these findings, enormous efforts have been made in utilizing pro-apoptotic compounds targeting anti-apoptotic Bcl-2 proteins in the hope to reintroduce the apoptotic potential in tumors and tumor environments (Lessene et al., 2008). In

this context, therapeutic strategies have already entered the clinical application with great promise in treating patients suffering hematologic malignancies (Brinkmann & Kashkar 2014).

Increased apoptosis and degenerative diseases

Unopposed or increased apoptosis is considered as a cause of tissue degeneration in aging and aging-associated diseases. In particular, increased apoptosis and the alterations of neuronal tissues such as Alzheimer's and Parkinson's disease are well described. *Alzheimer's disease* (AD) is the most common neurodegenerative disease, characterized by the progressive decline of neurons and synapses in the cerebral cortex and subcortical regions. AD is described by the accumulation of amyloid-ß peptide deposits in extracellular plaques and hyperphosphorylation of the microtubule-associated protein tau, eventually leading to the degeneration of affected regions. Apoptosis has been shown to be essential for the onset of the disease, especially in the caspase-mediated proteolysis of the amyloid precursor protein (APP) resulting in the aggregation of amyloid-ß peptides (Gervais et al., 1999; Garwood et al., 2011). Furthermore, Rohn and colleagues could demonstrate that by inhibiting apoptosis through overexpression of anti-apoptotic Bcl-2 in a mouse model of AD, the pathology could be drastically reduced (Rohn et al. 2008).

Parkinson's disease (PD) is the second most prevalent neurodegenerative disease and is characterized by a loss of specific dopaminergic neurons of the substantia nigra. PD has been linked to mutations in several genes necessary for efficient autophagic recovery of defective mitochondria and apoptosis regulation such as parkin and *(PTEN)-induced kinase 1* (PINK1) (Kitada et al., 1998; Valente et al., 2004). The E3-ligase parkin is involved in the ubiquitination and degradation of Bax and other pro-apoptotic proteins and hence acts as an anti-apoptotic sensitizer at the mitochondria, while PINK1 was shown to be necessary for the recruitment of parkin to mitochondria. PINK1 and parkin deletion were reported to enhance the levels of Bax translocation to the mitochondria and release of cytochrome c in the cytoplasm, resulting in constitutively elevated levels of active caspases (Wood-Kaczmar et al. 2008).

In addition to AD and PD, degenerative diseases caused by mitochondrial *oxidative phosphorylation* (OXPHOS) defects are also assumed to be associated with elevated apoptosis primarily in affected tissues with high energy demands (Breuer et al. 2013). In this context, mutations in nuclear DNA (nDNA) as well as mitochondrial DNA (mtDNA) encoding factors

involved in the respiratory chain are known to be causative in versatile severe degenerative states, premature aging phenotypes and premature mortality (Ylikallio & Suomalainen 2012). These findings highlight the role of mitochondrial integrity in the formation of degenerative states and raised attention to the impact of mitochondrial respiratory chain defects in the onset of a vast range of degenerative diseases.

The mitochondrial respiratory chain

According to the chemiosmotic theory proposed by Peter Mitchell in 1961, the demand for energy in form of ATP by cells and whole organisms is predominantly achieved by the translation of energy from energetic molecules by a concerted transfer of electrons (e^-) across an impermeable membrane, generating a chemical gradient which propels the synthesis of ATP (Mitchell 1961). This highly conserved process, termed oxidative phosphorylation, is located to the inner mitochondrial membrane (IMM) and composed of five large intermembrane complexes as well as the electron carriers ubiquinone and the inner membrane associated cytochrome c (Figure 1.2).

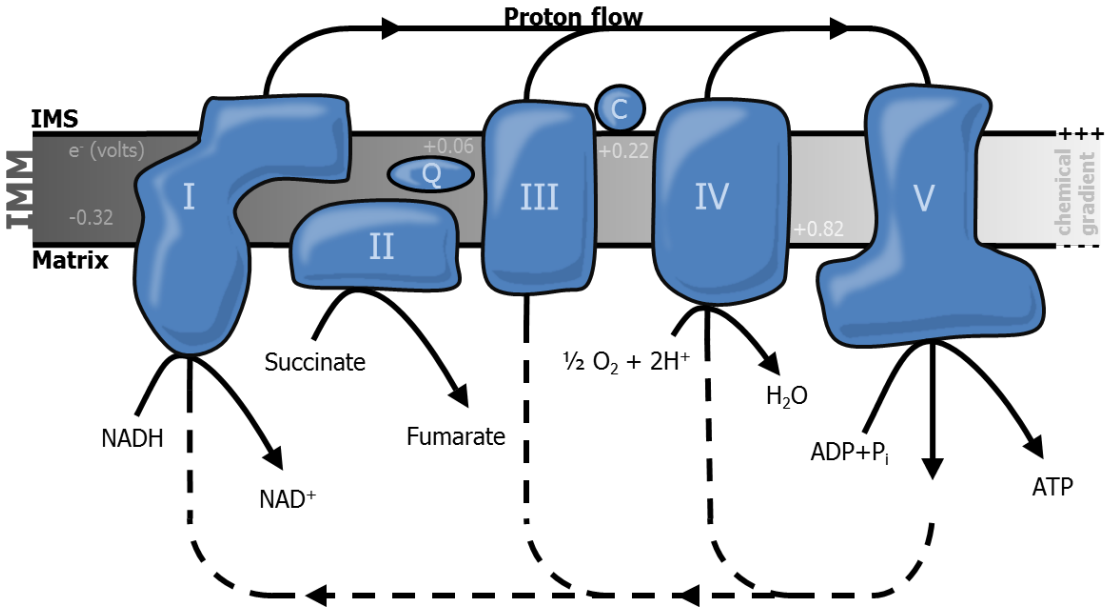

Figure 1.2 | Mitochondrial electron transport chain and oxidative phosphorylation

ATP production at the inner mitochondrial membrane (IMM) is coupled to the oxidation of nicotinamide adenine dinucleotide (NADH) at NADH-dehydrogenase (complex I) and flavin adenine dinucleotide

($FADH_2$) at Succinate dehydrogenase (complex II). Electrons (e^-) from complex I and II are transferred via reduction of ubiquinone (Q), which is then oxidized by Cytochrome c reductase (complex III). e^- are transferred to Cytochrome c oxidase (complex IV) by consecutive reduction and oxidation of cytochrome c (C) and finally reduce molecular oxygen and protons to water at the matrix-side of complex IV. The energy released during the electron transfer drives the translocation of protons from the matrix to the intermembrane space (IMS) across complex I, III and IV, generating a membrane potential across the IMM which drives the generation of ATP at the ATP synthase (complex V) by reflux of protons into the mitochondrial matrix. Electric potential differences are depicted at several steps of the respiratory chain. P_i, inorganic phosphate

The initial step of the oxidative phosphorylation cascade is the oxidation of the *tricarboxylic acid* cycle (TCA) metabolite *nicotinamide adenine dinucleotide* (NADH) by NADH-dehydrogenase (also referred to as complex I) (Hatefi & Stempel, 1969; Efremov et al., 2010; Hunte et al., 2010). Oxidation of NADH is the result of a higher redox-potential of the matrix-faced prosthetic group *flavin mononucleotide* (FMN), and transfer of two e^- to ubiquinone (or coenzyme Q_{10}) is accompanied by a still controversial mechanism of proton translocation across the IMM (reviewed in Brandt et al., 2003). A second entry point into the electron transport chain is provided by succinate-dehydrogenase (complex II) at which succinate is oxidized to fumarate by the prosthetic group *flavin adenine dinucleotide* (FAD) and e^- are subsequently transferred to ubiquinone by iron-sulfur clusters (Coles et al. 1979; Sun et al. 2005). Reduced ubiquinone is then oxidized by iron clusters within the heme group of cytochromes of cytochrome c reductase (complex III) (Hatefi et al., 1962; Xia et al., 1997), resulting in the dislocation of protons from the matrix side to the IMS and the transfer of e^- to cytochrome c (Leung & Hinkle 1975). In the last step, cytochrome c is reoxidized by cytochrome c oxidase (complex IV), repeatedly leading to the translocation of protons and finalizing the e^- cascade by the reduction of molecular oxygen and protons to water (Wikström, 1977; Tsukihara et al., 1996). As a result, the transformation of the electric potential of high-energetic metabolites originating from glycolysis, fatty acid oxidation and protein degradation generates a chemical gradient across the IMM known as *proton motive force* (PMF). This chemical gradient provokes a passive reflux of protons through the transmembrane channel of the F_O subunit of the ATP-synthase (complex V) (Soper et al., 1979; Ogawa & Lee, 1984), thus powering alternating conformational changes in the F_1 subunit of ATP-synthase and ultimately generating ATP from ADP and inorganic phosphate (Watt et al., 2010).

The mitochondrial respiratory chain and degenerative diseases

Mitochondria resemble their bacterial ancestry in terms of size, membrane architecture and dynamics. Most importantly, during their endosymbiotic evolution, intense expansive and reductive rearrangement of the mitochondrial proteome and massive transfer of the mitochondrial genome to the nucleus has left the mitochondrial network with traces of mtDNA (Nass & Nass, 1963; Clayton & Vinograd, 1967), which encode indispensable structural subunits of all OXPHOS complexes, except for complex II, as well as tRNAs and ribosomal RNAs (Anderson et al. 1981). In contrast to OXPHOS-defects resulting from mutations of nuclear encoded structural subunits and assembly factors or by autosomal mutations in nuclear encoded genes responsible for mtDNA maintenance, mitochondrial disorders resulting from sporadic or maternally inherited mutations of the mtDNA are always the result of threshold effects, given that the copy number of mtDNA varies between hundreds or thousands within a single cell (Elliott et al., 2008). While both, autosomal or x-linked nDNA and maternally inherited mtDNA mutations can manifest degenerative diseases at any age, the onset of age-associated diseases is predominantly the consequence of accumulated mutations or deletions of mtDNA within the lifetime of organisms (Lin et al., 2002; Kraytsberg et al., 2006).

Since the first descriptions of the molecular basis of disease-causing mutations of nuclear (Bourgeron et al., 1995) and mtDNA (Holt et al., 1988; Wallace et al., 1988) encoded OXPHOS proteins, the knowledge of degenerative diseases caused by mitochondrial dysfunction has widely expanded and to date more than 150 distinct genetic mitochondrial syndromes caused by approx. 300 mutations are known (Schon et al., 2012; Vafai & Mootha, 2012; www.mitomap.org/MITOMAP). The complex and diverse clinical appearance of distinct genetic mutations of OXPHOS complexes together with the bipartite origin of OXPHOS subunits has long time puzzled the understanding of mitochondrial disorders. Enormous advantages in molecular and cellular techniques like the standardized analysis of mtDNA mutations using *cellular hybrids* (cybrids) (King & Attardi 1989), the development of mouse models of nuclear encoded OXPHOS subunits and assembly factors (Vempati et al., 2009) and huge progress in genetic screenings have contributed to our current understanding of degenerative diseases (Ylikallio & Suomalainen 2012). The currently known mtDNA and nDNA encoded disease-causing structural subunits and assembly factor are summarized in Table 1.1.

Table 1.1: Common disease-encoding OXPHOS genes either encoding structural subunits (mtDNA and nDNA) or assembly factors (nDNA only) of the respective OXPHOS Complexes (not included: mutations in mitochondrial tRNAs and rRNAs).

Complex	Genetic defect	Genes
I	mtDNA	ND1-ND6
	nDNA structural gene	NDUFS1-NDUFS8; NDUFV1, 2; NDUFA1,2,11
	nDNA assembly factor	NDUFAF1,2; C6orf66;C8ORF38
II	nDNA structural gene	SDHA,SDHB,SDHC,SDHD
	nDNA assembly factor	SDHAF1,2
III	mtDNA	CYTB
	nDNA structural gene	UQCRB,UQCRQ
	nDNA assembly factor	BCS1L, TTG19
IV	mtDNA	COX1-3
	nDNA structural gene	COX6B1, COX4I2
	nDNA assembly factor	SURF1, SCO1 & 2, COX10, COX15, C2orf64
V	mtDNA	ATP6 & 8
	nDNA structural gene	ATP5E
	nDNA assembly factor	ATP12, TMEM70

Most OXPHOS defects are the result of nDNA mutations, given that the vast majority of OXPHOS complexes and assembly factors are encoded by the nucleus. Accordingly, defects in complex I, by far the largest of all OXPHOS complexes, represent most of the known OXPHOS defects (reviewed in Zhu et al., 2009). Mutations in nDNA and in mtDNA encoded OXPHOS subunits as well as in mitochondrial tRNAs and rRNAs precipitate many different and often fatal degenerative states like, amongst others, myopathy, cardiomyopathy, encephalopathy, hepatopathy and stroke (reviewed in Breuer et al., 2013). In spite of the diversity of OXPHOS defects-derived syndromes, most frequent and common to all OXPHOS complexes, especially complex I and IV, is *Leigh's syndrome* (LS) (Leigh 1951), a disease which is associated with lactic acidosis, muscle atrophy as well as bilateral, focal lesions of the basal ganglia and the brain-stem and early mortality (Baertling et al. 2014). *French Canadian Leigh syndrome* (LSFC), a type of LS frequently found in the region of Quebec and characterized by complex IV deficiency, is caused by mutations in the mitochondrial mRNA stability protein *leucine-rich pentatricopeptide repeat motif-containing* (LRPPRC) (Mootha et al., 2003; Debray et al., 2011).

Leber's hereditary optic neuropathy (LHON), a disease characterized by the degeneration of retinal ganglion cells, optic atrophy and loss of sight is the result of specific mtDNA mutations affecting complex I and, to lesser extent, complex III (Wallace et al., 1988; Bénit et al., 2009). Another disease shared by diverse mtDNA mutations is *mitochondrial encephalomyopathy, lactic acidosis and stroke-like episodes* (MELAS), a multisystem disorder affecting versatile tissues such as brain, muscle, heart and the endocrine system (Pavlakis et al., 1984) and mainly arises from a distinct mutation ("A3243G") in the mitochondrial $tRNA^{Leu}$ (Majamaa et al. 1998) as well as from mutations in complex I (Dimauro & Davidzon 2005) and mtDNA encoded subunits of complex IV (Manfredi et al., 1995; Rossmanith et al., 2008).

Degenerative diseases can also be the result of large scale deletions of mtDNA, first documented in patients suffering from *Kearns-Sayre syndrome* (KSS) by Moraes and colleagues in the early 1990s (Moraes et al., 1991; Moraes et al., 1992). More recent studies identified defects in proteins responsible for maintaining the mitochondrial nucleotide pool (Nishino et al., 1999), nucleotide transport (Kaukonen et al., 2000), and DNA replication (Spelbrink et al., 2001; Van Goethem et al., 2001) respectively, as source for large mtDNA deletions.

The mitochondrial respiratory chain and cell death

Within the last two decades, advantages in molecular techniques tremendously supported our understanding of the clinical features of degenerative diseases caused by defective OXPHOS and it became evident that tissue degeneration is associated with enhanced cell death. In LS, tissue degeneration mainly arises from necrotic cell death, though several investigations have linked the loss of cerebral tissue to enhanced apoptosis both histochemically (Formichi et al., 2004) or in cultured cybrids (Carrozzo et al. 2004), while a shift from apoptosis to necroptosis has also been reported (Quintana et al., 2010). Apoptotic cell death was also detected in peripheral blood lymphocytes of patients with LHON (Battisti et al. 2004), in cybrids containing different mtDNA mutations encoding complex I subunits ND1, 4 and 6 (Danielson et al. 2002; Ghelli et al. 2003), in patients suffering from KSS, MELAS and *chronic progressive external ophthalmoplegia* (CPEO) (Mirabella et al., 2000; Auré et al., 2006) and in patients with complex IV deficiency (Di Giovanni et al. 2001). Chemical inhibition of complex I in mice and utilizing complex I deficient cybrids revealed oxidative damage induced cell death, presumably by sensitizing affected cells to Bax-induced apoptosis (Perier et al. 2005). In addition, skin fibroblasts from patients suffering from complex V deficiency derived *neurogenic ataxia retinitis pigmentosa* (NARP) also displayed

superoxide-induced apoptosis (Geromel et al. 2001), while complex II deficiency seems to be generally linked to apoptotic demise by oxidative damage (reviewed in Grimm, 2013).

A growing contribution to our understanding of the correlation between defective OPXHOS compartments and increased apoptosis comes from increasing numbers of mouse models describing mitochondrial mutations. Roughly a decade ago the work of Trifunovic and colleagues and in parallel by Kujoth et al underlined the importance of mtDNA integrity in the generation of aging-associated degenerations. By generating mice with defective mtDNA-specific polymerase γ proofreading subunits, the authors could demonstrate that accumulating mtDNA mutations cause a loss of respiratory chain capacity, severe onset of premature aging and early lethality by tissue malfunction due to enhanced apoptosis (Trifunovic et al., 2004; Kujoth et al., 2005). In addition, knockout of the *mitochondrial transcription factor A* (TFAM) revealed massive apoptosis in knockout embryos and in the heart of TFAM tissue-specific knockout animals (Wang et al., 2001).

Furthermore, mouse models of defective respiratory chain subunits and assembly factors have highlighted the importance of OXPHOS integrity: Enhanced apoptosis preceding fatal hepatopathy was demonstrated in mice with a liver-specific knockout of COX10, an indispensable assembly factor of the prosthetic heme a of complex IV (Diaz et al., 2008). A muscle-specific knockout of COX10 revealed premature aging characteristics like weight loss, progressive myopathy and early mortality (Diaz et al., 2005). Embryonic lethality and early mortality was also linked to complex IV deficiency by the knockout of assembly factor SURF1 (Agostino et al., 2003) as well as for a knockout of SDHD, a membrane-anchoring subunit of complex II (Piruat et al. 2004). Knockout-mice of the complex I subunit NDUFS4 appeared healthy but developed fatal encephalomyopathy at the age of 5 weeks (Kruse et al. 2008).

Aim of the study

Apoptosis is a vital process in cell homeostasis and tissue-regeneration and has constantly been shown to be manipulated by diverse mitochondrial dysfunctions. Even though numerous findings in the recent years have shed light on the correlation between the decline of OXPHOS and the increase of cell death by apoptosis in various degenerative and aging-associated diseases (Breuer et al. 2013), the exact molecular mechanisms that trigger this mitochondrial dysfunction-associated tissue demise remain elusive.

Overwhelming generation of reactive oxygen species (ROS) has been long-standing associated with defective mitochondrial respiration, though the causality of excessive ROS generation and the decline of mitochondrial respiratory activity is still heavily debated. However, oxidative stress has often been implicated in the onset of OXPHOS-degenerative states as well as aging and aging-associated diseases (Cui et al., 2012). In this context, the present work aims to dissect the role of the distinct complexes of the mitochondrial respiratory chain towards oxidative stress induced apoptosis and tries to substantiate our understanding of the molecular mechanisms underlying OXPHOS-dysfunction induced enhanced apoptosis.

Material and Methods

Cell culture

Human cell lines Hela (CCL-2, obtained from American Type Culture Collection (ATCC), Rockville, MD, USA), Hela Bcl-2 (Kashkar et al.,2005), 143B control and $143B_{\Delta COX}$ (gift from R. Wiesner, Cologne, Germany) as well as adult murine fibroblasts of COX10 knockout mice (gift from C. Moraes, Miami, FL, USA) and murine embryonic fibroblasts (MEFs) of Bax and Bak single and Bax/Bak double-knockout mice (gift from A. Villunger, Innsbruck, Austria) were cultured in Dulbecco's modified Eagle's medium (DMEM, Gibco (Life Technologies), Darmstadt, Germany), supplemented with 10% fetal calf serum (FCS, Gibco (Life Technologies), Darmstadt, Germany), 100 µ/ml streptomycin and 100 U/ml penicillin (Biochrom (Merck), Darmstadt, Germany). DMEM of $143B_{\Delta COX}$, COX10 knockout fibroblasts or mammalian cell lines under conditions of chemical suppression of the mitochondrial respiratory chain (RC) was supplemented with 1mM sodium pyruvate (Biochrom (Merck), Darmstadt, Germany) and 50µg/ml uridine (Sigma-Aldrich, Seelze, Germany).

Chemicals and reagents

All chemicals were purchased from Merck (Darmstadt, Germany), Roth (Karlsruhe, Germany) and Sigma-Aldrich (Seelze, Germany), unless indicated otherwise. Staurosporine, zLEHD-fmk, zIETD-fmk and zVAD-fmk were obtained from Enzo Life Sciences (Lörrach, Germany). Rotenone, 3-nitropropionic acid (3-NP), antimycin A, KCN, oligomycin, and H_2O_2 were purchased from Sigma-Aldrich (Seelze, Germany).

Measurement of oxygen consumption

Measurement of oxygen consumption was performed with a Clark-like oxygen electrode system (Hansatech Instruments, Norfolk, UK). $4x10^6$ cells were diluted in Buffer E and placed in a water-filled, air-saturated chamber at 37°C. Water-dissolved oxygen was reduced by the addition of trace amounts of dithionite ($Na_2S_2O_4$). Oxygen consumption under conditions of chemical inhibition of the respective respiratory chain complexes was recorded, related to total cell number and expressed as femtomoles O_2 per cell per minute.

Table 2.1: Buffers for oxygen consumption

Buffer E	300 mM Mannitol; 5 mM $MgCl_2$; 10 mM KCl; 10 mM KH_2PO_4, pH 7.4; 1mg/ml bovine serum albumin, fatty acid free

Table 2.2: Respiratory chain-inhibitors and concentrations

Compound	RC-complex	Concentration (half-maximum; maximum)
Rotenone	NADH dehydrogenase (Complex I)	50; 100 [nM]
3-NP	Succinate dehydrogenase (Complex II)	1; 2 [mM]
Antimycin A	Cytochrome c reductase (Complex III)	50; 100 [µM]
KCN	Cytochrome c oxidase (Complex IV,COX)	0,5; 1 [mM]
Oligomycin	ATP synthase (Complex V)	0,5; 1 [µM]

DNA constructs and siRNA-mediated knockdown

For the construction of human ceramide synthase (CerS) GFP fusion proteins, open reading frames encoding human ceramide synthase 3 and 6 were amplified by PCR with appropriate restriction sites and cloned into pEGFP-N3 vector (Clontech, Saint-Germain-en-Laye, France). For the generation of $CerS6_{R131A}$, site-directed mutagenesis PCR was performed on pEGFP-CerS6. Cells were transfected with TurboFect transfection reagent (Thermo Scientific, Rockford, IL, USA) according to manufacturer's manual and incubated for at least 24h.

Table 2.3: Primers for DNA constructs

Construct	Primer ('5-3')
CerS3 forward (5'-EcoRI)	GATCGAATTCATGTTTTGGACGTTTAAAGAATGGTTCTG
CerS3 reverse (3'-BamHI)	GATCGGATCCATGGCCATGCTGGCCATT
CerS6 forward (5'-EcoRI)	GATCGAATTCATGGCAGGGATCTTAGCC
CerS6 reverse (3'-BamHI)	GATCGGATCCATCATCCATGGAGCAGGAGCC
$CerS6_{R131A}$ sense	TTCTGTGAGAGCATGTGGAGATTT
$CerS6_{R131A}$ anti-sense	GGCCGTCAGCGTGCTTGGCTTCTCCTG

For siRNA mediated knockdown of human CerS6 as well as murine CerS6 (mCerS6), suitable amounts of cells were transfected with 100 pmol/ml siRNA using Lipofectamine™ RNAimax transfection reagent (Life Technologies, Darmstadt, Germany) and incubated for 48h before cytotoxic treatment. All siRNAs were purchased from Eurofins MWG Operon (Ebersberg, Germany).

Table 2.4: siRNAs used in this work

siRNA	Sequence	Supplier	Reference
CerS6	5'- AAGGUCUUCACUGCAAUUACATT-3'	Eurofins MWG Operon (Ebersberg, Germany)	Senkal et al, 2010
mCerS6	5'- GAGGAGAAACCCAGCACUC-3'	Eurofins MWG Operon (Ebersberg, Germany)	-
SCR (human)	Allstars Neg. siRNA	Qiagen (Hilden, Germany)	-
SCR (murine)	Allstars Neg. siRNA	Qiagen (Hilden, Germany)	-

Cell death

Cell death was measured by trypan blue exclusion using an automated cell counter (Countess™, Life Technologies, Darmstadt, Germany) according to manufacturer's instructions. In brief, approx. 0.75-1.5x10^5 cells were seeded in 24-well chambers and incubated under desired conditions. Before counting, cells were briefly detached with trypsin and diluted to appropriate working concentrations. Cell suspension was then diluted with trypan blue in a ratio of 1:1 (v/v) and dead cells were measured.

Measurement of superoxide formation

For immunofluorescence analysis of superoxide (O_2^-) formation, MitoSox™ Red mitochondrial superoxide kit (Life Technologies, Darmstadt, Germany) was used according to manufacturer's instructions. In brief, 3x10^5 cells were seeded on sterile glass bottom live cell dishes (Greiner Bio-One, Frickenhausen, Germany), incubated with 5 µM MitoSox™ reagent working solution and washed three times with warm HBSS/Ca/Mg buffer (Life Technologies, Darmstadt,

Germany). Samples were analyzed with an Olympus Flowview 1000 confocal microscope (Olympus, Hamburg, Germany). Additionally, $3x10^5$ Hela cells were incubated with 5 µM MitoSox™ reagent working solution and washed three times with warm HBSS/Ca/Mg buffer and analyzed by flow cytometry (BD FACSCalibur™, BD Biosciences, Heidelberg, Germany).

Sample preparation and immunoblotting (IB)

Whole cell lysates were prepared by incubating cell pellets in CHAPS lysis buffer on ice for 20 min and subsequent centrifugation at 14.000 x g for 20 min at 4°C to recover the supernatant. To obtain cytosolic extracts, cells were incubated for 20 min in ice-cold HEP buffer following mechanical disruption by repeated passaging (x12-15) through a 26 x G 1/2`` needle, the supernatant was recovered after centrifugation at 20.000 x g for 20 min at 4°C. For Western blotting, equal amounts of protein, determined by BCA protein assay (Thermo Scientific, Rockford, IL, USA) were prepared in 1x Laemmli buffer containing 4% ß-mercaptoethanol, separated by SDS-PAGE and transferred onto nitrocellulose membranes (Protran BA85, GE Healthcare, Freiburg, Germany). After blocking and appropriate incubation in primary and secondary antibodies, protein signals were visualized by enhanced chemiluminescence (ECL; Thermo Scientific, Rockford, IL, USA).

Table 2.5: Primary and secondary antibodies (IB)

Antibody	Isotope	Supplier
ß-Actin	mouse, monoclonal	Sigma-Aldrich (Seelze, Germany)
Bak (clone G317-2)	mouse, monoclonal	BD Bioscience (Heidelberg, Germany)
Bax (human)	rabbit, polyclonal	BD Bioscience (Heidelberg, Germany)
Bax, active (clone 6A7)	mouse, monoclonal	BD Bioscience (Heidelberg, Germany)
Bcl-xL (clone 5H46)	mouse, monoclonal	Cell Signaling (Frankfurt a.M., Germany)
Bcl-2 (human,clone 4D7)	mouse, monoclonal	BD Bioscience (Heidelberg, Germany)
COXI (clone 1D6E1A8)	mouse, monoclonal	Mitoscience/Abcam (Cambridge, UK)
Cytochrome C (clone 7H8, 2C12)	mouse, monoclonal	BD Bioscience (Heidelberg, Germany)
Caspase 3 (clone 8G10)	rabbit, monoclonal	Cell Signaling (Frankfurt a.M., Germany)
Caspase 9 (human)	rabbit, polyclonal	Cell Signaling (Frankfurt a.M., Germany)

Caspase 9 (mouse)	rabbit, polyclonal	Cell Signaling (Frankfurt a.M., Germany)
Ceramide Synthase 6	mouse, polyclonal	Abnova (Heidelberg, Germany)
GAPDH (clone D16H11)	rabbit, monoclonal	Cell Signaling (Frankfurt a.M., Germany)
Mcl-1	rabbit, polyclonal	Cell Signaling (Frankfurt a.M., Germany)
Anti-mouse IgG HRP-linked	goat	Sigma-Aldrich (Seelze, Germany)
Anti-rabbit IgG HRP-linked	goat	Sigma-Aldrich (Seelze, Germany)

Table 2.6: Buffers for sample preparation and immunoblotting

Antibody dilution buffer	50 mM Tris, pH 7.6; 150 mM NaCl; 0,1% Tween-20; 5% BSA
Blocking buffer	10 mM Tris-Hcl, pH 7.4-7.6; 150 mM NaCl; 5% milk powder; 2% BSA; 0.1% Tween-20
Blot transfer buffer	25 mM Tris-HCl; 190 mM glycine; 20% methanol
CHAPS lysis buffer	10 mM HEPES, pH 7.4; 150 mM NaCl; 1% CHAPS; protease inhibitor
HEP buffer	20 mM HEPES, pH 7.5; 10 mM KCl; 1.5 mM $MgCl_2$; 1 mM EDTA; 10 µM cytochalasin B; 1 mM DTT; protease inhibitor
Laemmli sample buffer (5x)	0.6 M Tris-HCl, pH 6.8; 144 mM SDS; 25% glycerol; 0.1% bromophenol blue; 5% ß-mercaptoethanol
SDS running buffer	190 mM glycine; 20 mM Tris; 0.1% SDS
S-PBS	120 mM NaCl; 10 mM NaH_2PO_4; 30 mM K_2HPO_4, pH 7.6

Immunoprecipitation (IP) of active Bax

100 µg of whole cell lysates were brought to a final volume of 500 µl with CHAPS lysis buffer containing 150mM KCl and incubated with 2 µg of monoclonal, active Bax- specific antibody 6A7 over night at 4°C. The antigen-antibody complex was immobilized by the addition of GammaBind-G-Sepharose (GE Healthcare, Freiburg, Germany) and subsequent gentle rotation for 2h at 4°C. Samples were washed twice with CHAPS/ 150mM KCl and the complexes were pelleted by centrifugation at 500 x g for 1 min. The resolved pellet was washed twice with CHAPS/ 150 mM KCl and further subjected to SDS-Page and western blotting.

Lipid analysis

Total amount of cellular sphingolipid levels were determined from whole cell homogenates of at least $1x10^6$ cells. For ceramide synthase activity measurement, $2,5x10^6$ cells were incubated with 2 µM C_{17}-sphinganine (Avanti Polar Lipids, Alabaster, AL, USA) for 2h prior to cell homogenization. Lipids were extracted in methanol/chloroform 2:1 (v/v) overnight at 48°C, purified and analyzed by Liquid Chromatography coupled to Electrospray Ionization Tandem Mass Spectrometry (LC-ESI-MS/MS) by Dr. Susanne Brodesser at the Cecad Lipidomics Facility.

Activity of neutral and acid sphingomyelinase (n/aSMase) was measured by Katja Krönke-Wiegmann from crude cytosolic extracts (nSMase) or total cell lysates (aSMase) of at least $3x10^6$ cells in appropriate buffer using 0.2 µCi/ ml [^{14}C]sphingomyelin (Amersham/ GE Healthcare, Freiburg, Germany). The amount of sphingolipid hydrolysis derived phosphorylcholin was measured by thin layer chromatography (TLC) and scintillation counting (Zinsser Analytic, Frankfurt a.M., Germany)

Table 2.7: Buffers for lipid analysis

nSMase sample buffer	20 mM HEPES, pH 7.4; 10 mM $MgCL_2$; 2 mM EDTA; 5 mM DTT, 0.1 mM Na_3VO_4; 0.1 mM Na_2MoO_4; 30 mM p-nitrophenylphosphate; 10 mM ß-glycerophosphate; 750 µM ATP; 1 mM PMSF; 10 µM leupeptin; 10 µM pepstatin; 0.2% Triton X-100
aSMase sample buffer	0.2% Triton X-100
nSMase activity buffer	20 mM HEPES; 1 mM $MgCl_2$, pH 7.4
aSMase activity buffer	250 mM sodium acetate; 1 mM EDTA, pH 5.0

Fluorescence microscopy

For immunofluorescence (IF) analyses of Bax activation and cytochrome c release, $3x10^5$ Hela cells were transfected with 1 µg of the particular pEGFP-N3 constructs and incubated for 24h before subjection to H_2O_2 for 4h. Cells were washed twice with PBS, fixed in 3% paraformaldehyde and simultaneously permeabilized and blocked with blocking buffer for 30 min. Cells were incubated with monoclonal active Bax 6A7 antibody over night at 4°C. Cells were

washed three times for 10 min with washing buffer and incubated with Alexa Fluor™ 647 secondary antibody for 1h at room temperature. Cells were washed three times with washing buffer for 10 min. For staining of cytochrome c, directly Alexa Fluor™ 555 labeled cytochrome c antibody was utilized according to manufacturer's instructions. Cells were washed three times with washing buffer for 10 min and Dapi was added to the second washing step for nuclei staining. Samples were mounted onto cover slides using Mowiol mounting medium and examined with a spinning disk confocal microscope (Perkin Elmer, Rodgau, Germany).

Table 2.8: Primary and secondary antibodies (IF)

Antibody/Compound	Isotope	Supplier
Cytochrome C Alexa Fluor™ 555	mouse, monoclonal	BD Bioscience (Heidelberg, Germany)
Anti-mouse Alexa Fluor™ 647	goat	Life Technologies (Darmstadt, Germany)
Dapi	-	Life Technologies (Darmstadt, Germany)

Statistical Analysis

Data are presented as mean of at least three independent experiments. Standard deviation (SD) and standard error of the mean (SEM) were calculated as indicated in the figures. Statistical significance was calculated by two tailed unpaired student's t-test.

Software

Vector NTI	(Plasmids)
FlowJo	(Flow cytometry)
Photoshop CS2	(IF, IB)
ImageJ, Volocity	(IF)
Illustrator CS2	(data processing)

Results

Chemical inhibition of cytochrome c oxidase selectively enhances ROS-induced cell death

The decline of mitochondrial respiratory capacity and the incidence of cellular death resulting in tissue degeneration have been extensively described (Breuer et al. 2013). However, it is still unclear how excessive apoptosis within a degenerative tissue impacts on tissue damage caused by mitochondrial dysfunction. To investigate how specific alterations of the mitochondrial respiratory chain (RC) as well as ATP-synthase impact on apoptosis, the activity of each of the five oxidative phosphorylation (OXPHOS) complexes was chemically inhibited in Hela cells (Figure 3.1). Oxygen consumption was monitored as a read-out for the efficacy of the chemical inhibition of OXPHOS complexes, revealing a reduction in respiration between 15 and 24% of untreated conditions (Figure 3.1 B). Inhibitor concentrations were chosen based on maximal efficacy without cytotoxic side effects in a period of 48h as measured by trypan blue exclusion assay (Figure 3.1 A).

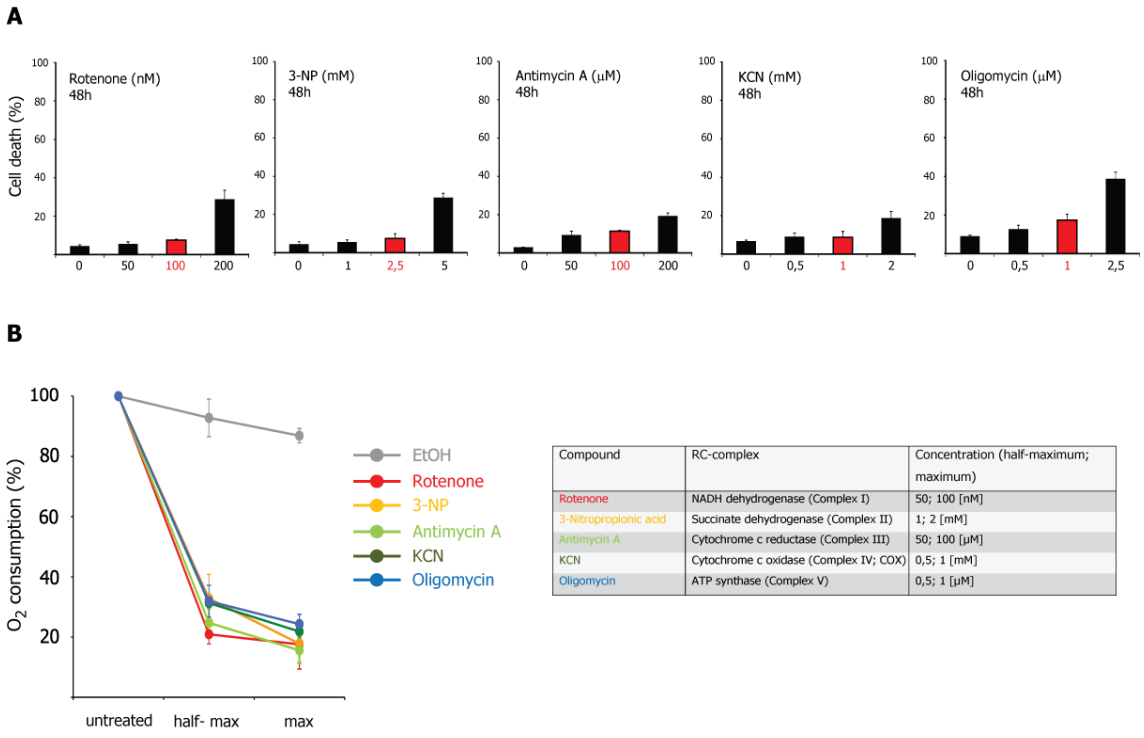

Compound	RC-complex	Concentration (half-maximum; maximum)
Rotenone	NADH dehydrogenase (Complex I)	50; 100 [nM]
3-Nitropropionic acid	Succinate dehydrogenase (Complex II)	1; 2 [mM]
Antimycin A	Cytochrome c reductase (Complex III)	50; 100 [µM]
KCN	Cytochrome c oxidase (Complex IV; COX)	0,5; 1 [mM]
Oligomycin	ATP synthase (Complex V)	0,5; 1 [µM]

Figure 3.1 | Chemical inhibition of mitochondrial respiratory chain complexes

(A) Hela cells were incubated with increasing concentrations of the respective OXPHOS inhibitors and cell death was assessed after 48h by trypan blue exclusion. Error bars represent mean ± SEM (n=3).

(B) Hela cells were incubated with two concentrations of specific inhibitors as listed in the table and oxygen consumption rate was instantly measured with a Clark-like oxygen electrode system. EtOH (vehicle) concentration was 1 and 2% (v/v), respectively. Error bars represent mean ± SEM of at least four experiments.

Oxidative damage within an aging tissue (e.g. by mitochondrial dysfunction) has been considered as one of the central mechanisms causing tissue degeneration (Turrens, 2003; Balaban et al., 2005; Sena & Chandel, 2012). Therefore, we first investigated whether the inhibition of OXPHOS complexes interferes with the susceptibility of cells towards oxidative stress by exposing Hela cells to RC inhibitors together with increasing amounts of H_2O_2 (Figure 3.2). In striking contrast to the inhibition of all other OXPHOS complexes, inhibition of cytochrome c oxidase (COX/complex IV) revealed a dramatic increase in susceptibility to H_2O_2 in a dose dependent manner (Figure 3.2).

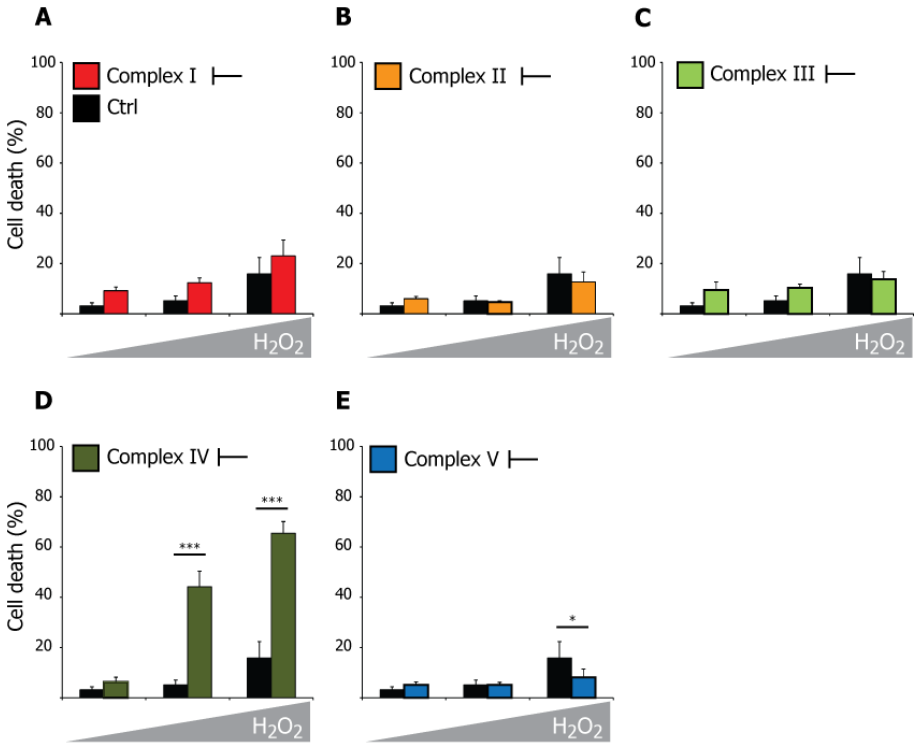

Figure 3.2 | Inhibition of cytochrome c oxidase enhances H_2O_2-induced cell death

Hela cells were left untreated or treated with OXPHOS complex inhibitors; (A) rotenone [100 nM], (B) 3-nitropropionic acid [2 mM], (C) antimycin A [100 µM], (D) KCN [1 mM], (E) oligomycin [1 µM]. After 24h, cells were subjected to increasing concentrations of H_2O_2 [0; 50; 150 µM] and cell death was assessed after 20h by trypan blue exclusion. Error bars represent mean ± SEM (n=6).Statistical significance was measured by two tailed unpaired t-test (including all following figures). *p<0.05, ***p<0.001

Importantly, the inhibition of the OXPHOS complexes did not interfere with susceptibility to the well-known apoptosis-inducer staurosporine (STS) (Figure 3.3).

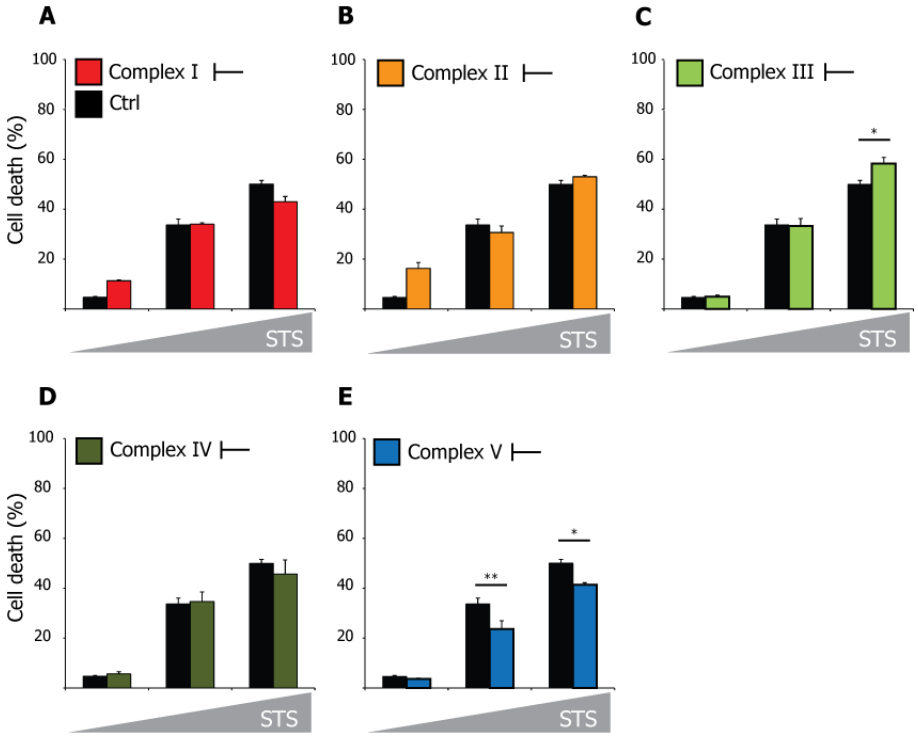

Figure 3.3 | Inhibition of RC complexes does not influence STS-induced cell death

Hela cells were left untreated or treated with OXPHOS complex inhibitors; (A) rotenone, (B) 3-nitropropionic acid, (C) antimycin A, (D) KCN, (E) oligomycin as described in Figure 3.2. After 24h, cells were subjected to increasing concentrations of STS [0; 25; 50 nM] and cell death was assessed after 20h by trypan blue exclusion. Error bars represent mean ± SEM (n=3). *p<0.05, **p<0.01

Notably, in contrast to H_2O_2 treatment, inhibition of complex V slightly reduced the cytotoxic effect of STS (Figure 3.3 E). Taken together, these data indicate that the selective inhibition of COX specifically leads to an increased susceptibility towards oxidative stress.

Cytochrome c oxidase dysfunction enhances oxidative stress-induced apoptosis

To test whether the increased susceptibility to oxidative stress upon COX inhibition was due to enhanced apoptosis, we measured cell death in the presence of caspase inhibitors (Figure 3.4). The efficacy of the caspase inhibitors was examined by analyzing the proteolytic activation of the executioner caspase 3 upon treatment with TRAIL or STS (Figure 3.4 B). Whereas the inhibition of caspase 8 by zIETD potently inhibited TRAIL-induced caspase 3 processing, the exposure to zLEHD, a potent caspase 9 inhibitor, only diminished STS-induced caspase 3-activation. The exposure of KCN-treated Hela cells to the pan-caspase inhibitor zVAD completely abolished susceptibility to H_2O_2, indicating a central role of caspase activation in oxidative stress-induced cell death upon COX dysfunction (Figure 3.4 A). In order to elucidate the involvement of the extrinsic or the intrinsic apoptotic cascade, the initiator caspases 8 or 9 were specifically inhibited (Figure 3.4 A). While the inhibition of caspase 9 by zLEHD efficiently reduced cell death in KCN-treated Hela cells upon H_2O_2 treatment (Figure 3.4 A), the inhibition of caspase 8 by zIETD revealed significant, but weak reduction of susceptibility towards oxidative stress. These results indicate a pivotal role of the intrinsic apoptotic machinery in this process.

The central and irreversible event in the intrinsic apoptotic pathway is the release of cytochrome c (Cyt c) from the mitochondrial intermembrane space (IMS). Indeed, H_2O_2–induced cell death in KCN-treated Hela cells was accompanied by the release of cytochrome c from mitochondria and the processing of caspase 9 (Figure 3.4 C). Mitochondrial outer membrane permeabilization (MOMP) and the subsequent release of cytochrome c from the mitochondrial IMS are tightly regulated by Bcl-2 proteins. In particular, Bax conformational changes represent an immediate early response to apoptotic stress, followed by the insertion of activated Bax into the mitochondrial outer membrane and pore formation (Martinou & Youle 2011), and the conformational changes allow for the specific detection of active Bax (Hsu & Youle 1998). Whereas undetectable in control Hela cells, KCN-treated Hela cells showed Bax-activation upon treatment with H_2O_2 (Figure 3.4, lower panel), further confirming the involvement of the mitochondrial apoptotic pathway in COX dysfunction-induced susceptibility to oxidative stress.

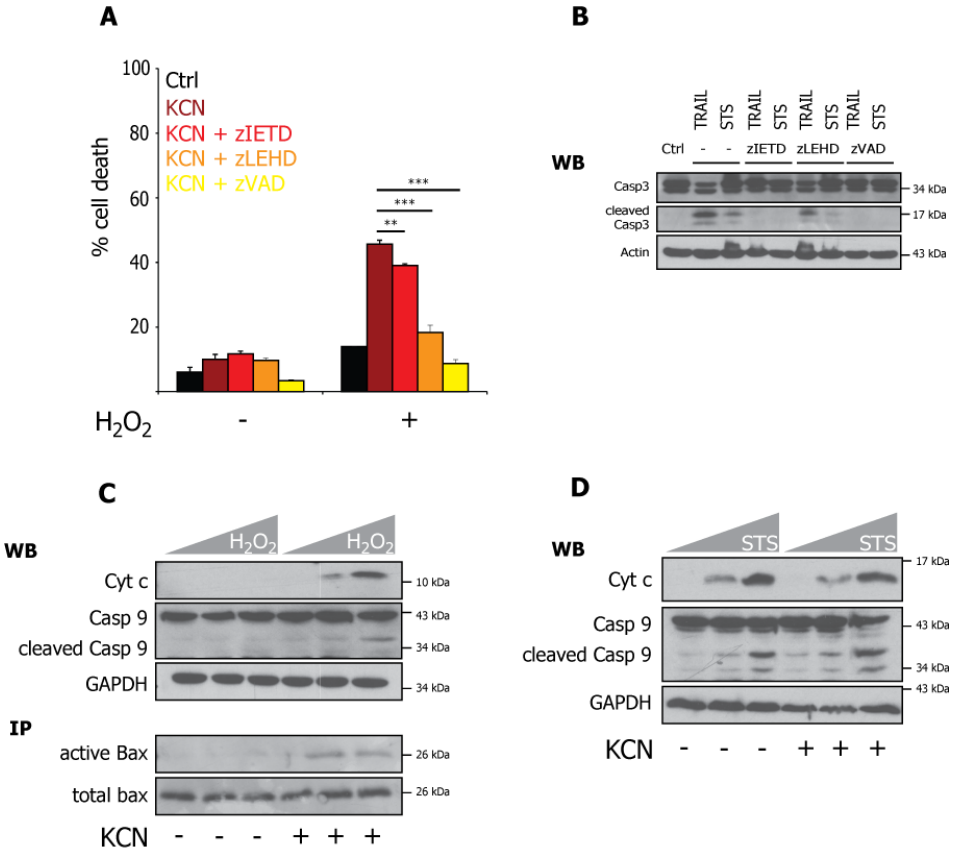

Figure 3.4 | Inhibition of cytochrome c oxidase accelerates mitochondrial apoptosis in response to H_2O_2

(A) Hela cells were treated with KCN [1 mM] or left untreated and incubated with caspase 8 inhibitor zIETD-fmk [2 µM], caspase 9 inhibitor zLEHD-fmk [2 µM] or caspase family inhibitor zVAD-fmk [20 µM] and treated with H_2O_2 [50 µM] for 20h. Cell death was assessed by trypan blue exclusion. Error bars represent mean ± SEM (n=3). **p<0.01, ***p<0.001

(B) Hela cells were incubated with caspase inhibitor as in (A) and treated with TRAIL [5 µg/ml] or STS [100 nM]. After 6h, cleavage of caspase 3 was analyzed in total cell lysates by Western blotting.

(C) Hela cells were left untreated (-) or treated (+) with KCN [1 mM] 24h before addition of H_2O_2 [0; 50; 150 µM]. After 6h, release of cytochrome c was analyzed in cytosolic fractions by Western blot. For detection of caspase 9 cleavage, total cell lysates were analyzed after 12h by Western blot. Activated Bax was immunoprecipitated and analyzed with corresponding Bax of total cell lysates by Western blot.

(D) Hela cells were left untreated (-) or treated (+) with KCN [1 mM] for 24h before addition of STS [0; 25; 50 nM]. After 6h, release of cytochrome c and cleavage of caspase 9 was analyzed in cytosolic fractions by Western blot.

Consistent with the data shown in Figure 3.3, we could demonstrate that COX-deficiency did not influence STS-induced cytochrome c release or the activation of caspase 9 (Figure 3.4 D), underlining the specific mode of the COX dysfunction-induced accelerated mitochondrial apoptosis in response to oxidative stress.

Even though the causality of ROS increase, mtDNA damage and RC dysfunction is still debated, there is a general consensus that increased ROS mainly arises from defects in complex I and/or complex III, while COX is of minor importance (Kwong et al., 2007; Orrenius et al., 2007; Diaz et al., 2012). To investigate if the sensitivity of COX-deficient Hela cells to oxidative stress is due to elevated basal levels of ROS within mitochondria, we measured the generation of mitochondrial superoxide (O_2^-) in the mitochondrial matrix. No difference to DMSO treated control Hela cells could be detected after treatment with KCN, while rotenone, the inhibitor of complex I, strongly induced superoxide production as shown by FACS-analysis and microscopic imaging (Figure 3.5 C and D).

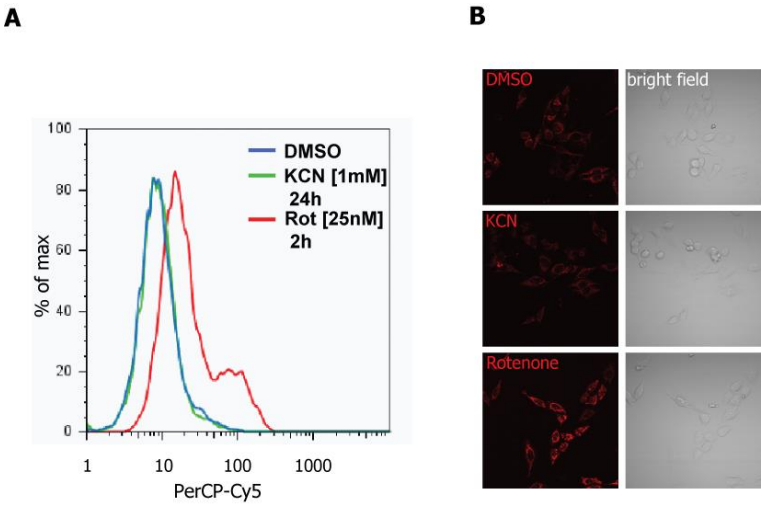

Figure 3.5 | COX does not elevate basal ROS levels

(A) Hela cells were treated with KCN [1 mM], rotenone [25 nM] or vehicle for 24h or 2h and the generation of O_2^- was visualized with MitoSox™ Red by flow cytometry. DMSO = 2% (v/v)

(B) Hela cells were treated with KCN [1 mM], rotenone [25 nM] or vehicle for 2h and the generation of O_2^- was analyzed with MitoSox™ Red by confocal microscopy. DMSO = 2% (v/v)

To further investigate the involvement of the mitochondrial apoptotic pathway in KCN-treated Hela cells towards oxidative stress the susceptibility of Bax and/or Bak-deficient murine embryonic fibroblasts (MEFs) and Hela cells stably overexpressing anti-apoptotic Bcl-2 (Hela Bcl-2) was analyzed (Figure 3.6-7). In line with our data summarized in Figure 3.4, the single deletion of Bax or Bak or double deletion of Bax/Bak (Figure 3.6 A and C) as well as the overexpression of Bcl-2 (Figure 3.7 A) completely diminished the COX dysfunction-induced susceptibility to oxidative stress. Congruently, in BB DKO (Figure 3.6 B) and Hela Bcl-2 (Figure 3.7 B) cells the inhibition of COX did not result in the release of cytochrome c upon treatment with H_2O_2, indicating the involvement of the Bcl-2 protein family in this process.

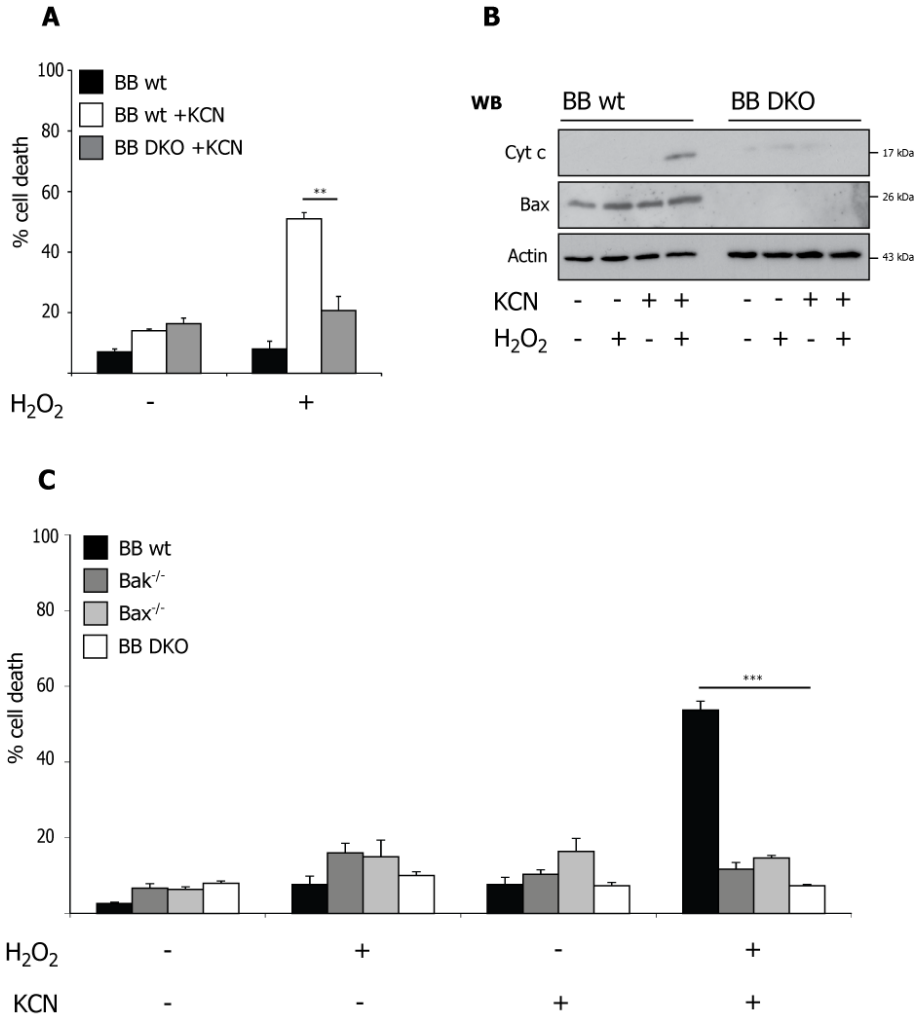

Figure 3.6 | COX dysfunction-induced susceptibility to H_2O_2 is dependent on pro-apoptotic Bax and Bak

(A) MEF isolated from wild type (BB wt) or Bax/ Bak double knockout (BB DKO) mice were left untreated or treated with KCN [200 µM]. After 24h, cells were left untreated (-) or treated (+) with H_2O_2 [100 µM] and cell death was assessed by trypan blue exclusion after 18h. Error bars represent mean ± SEM (n=3).
(B) MEF isolated from wild type (BB wt) or Bax/ Bak double knockout (BB DKO) mice were left untreated (-) or treated (+) with KCN [200 µM] 24h before addition (+) of H_2O_2 [100 µM]. After 6h, release of cytochrome c was analyzed in cytosolic fractions by Western blot.
(C) MEF isolated from wild type (BB wt), single and double knockout of Bax/ Bak (BB DKO) mice were left untreated (-) or treated (+) with KCN [200µM]. After 24h, cells were treated (+) with H_2O_2 [50 µM] and cell death was assessed by trypan blue exclusion after 18h. Error bars represent mean ± SEM (n=3) **p<0.01, ***p<0.001

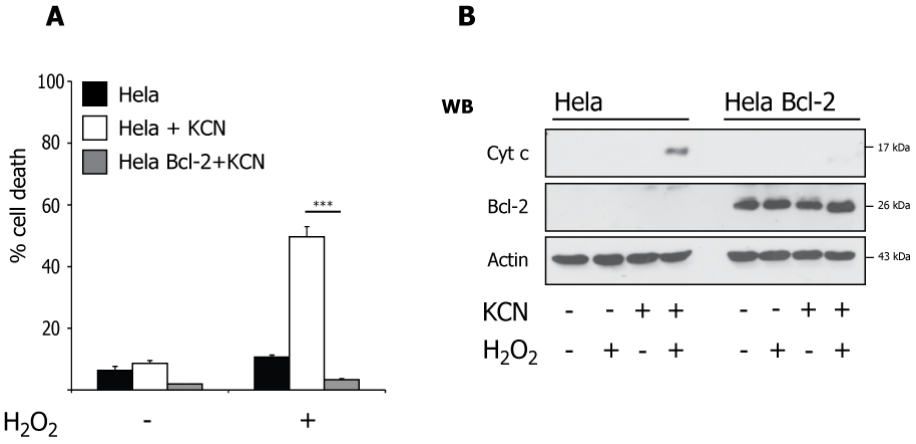

Figure 3.7 | Bcl-2 overexpression antagonizes COX dysfunction induced susceptibility to ROS

(A) Hela or Hela Bcl-2 cells were left untreated or treated with KCN [1 mM]. After 24h cells were left untreated (-) or treated (+) with H_2O_2 [150 µM] and cell death was assessed by trypan blue exclusion after 18h. Error bars represent mean ± SEM (n=3). ***p<0.001
(B) Hela or Hela Bcl-2 cells were left untreated (-) or treated (+) with KCN [1 mM] 24h before addition (+) of H_2O_2 [150 µM]. After 6h, release of cytochrome c was analyzed in cytosolic fractions by Western blot.

Taken together, our data suggest that COX-deficiency induces apoptotic cell death towards oxidative stress. This susceptibility is dependent on the induction of MOMP and regulated by the Bcl-2 protein family.

mtDNA depletion-derived COX deficiency enhances mitochondrial apoptosis in response to oxidative stress.

The naturally occurring causes for mitochondrial respiratory chain dysfunction are predominantly somatic or inherited mutations in the mtDNA and nuclear DNA (Schon et al., 2012). In order to substantiate the previous findings we had obtained by chemically inhibiting COX, we investigated two cell lines with genetically derived COX-deficiency towards their susceptibility to oxidative stress.

The human osteosarcoma cybrid cell line $143B_{\Delta COX}$ contains a homoplasmic G→A transition at position 6930 of the mtDNA, leading to a loss of the last 170 amino acids of cytochrome c oxidase subunit I (COXI) and to the disassembly of COX (Bruno et al. 1999). Similar to KCN-treated Hela cells, the $143B_{\Delta COX}$ cell line displayed a dramatic susceptibility to H_2O_2 (Figure 3.8). Furthermore, although highly susceptible to oxidative stress, $143B_{\Delta COX}$ cells were not increasingly susceptible to STS (Figure 3.8 B).

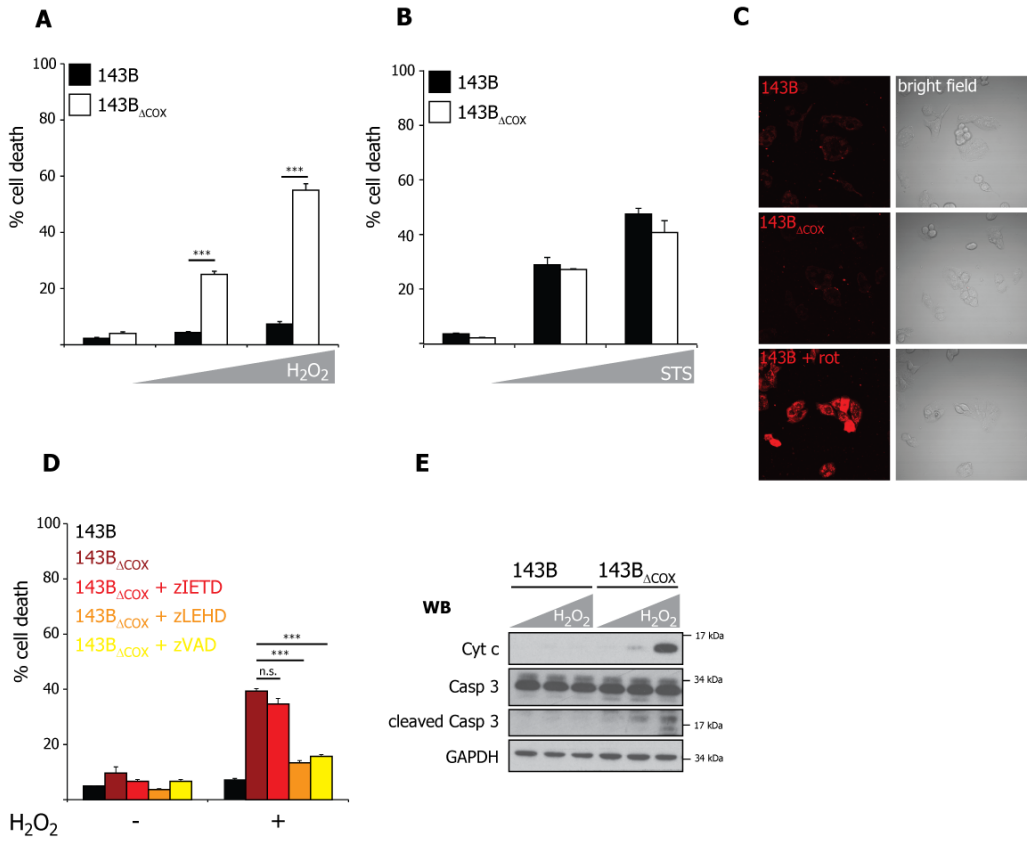

Figure 3.8 | 143B$_{\Delta COX}$ cybrids display enhanced susceptibility to oxidative stress

(A & B) 143B and 143B$_{\Delta COX}$ cells were treated with increasing concentrations of (A) H_2O_2 [0; 100; 250 µM] or (B) STS [0; 50; 100 nM] and cell death was assessed by trypan blue exclusion after 20h (H_2O_2, STS). Error bars represent mean ± SEM (n=3). ***p<0.001

(C) 143B and 143B$_{\Delta COX}$ cells were left untreated or treated with rotenone [25 nM] for 3h as indicated and the generation of O_2^- was analyzed with MitoSox^{TM} Red by confocal microscopy.

(D) 143B and 143B$_{\Delta COX}$ cells were left untreated or treated with caspase 8 inhibitor zIETD-fmk [2 µM], caspase 9 inhibitor zLEHD-fmk [2 µM] or caspase family inhibitor zVAD-fmk [20 µM] and subjected to H_2O_2 [150 µM] for 18h. Cell death was assessed by trypan blue exclusion. Error bars represent mean ± SEM (n=3). ***p<0.001

(E) 143B and 143B$_{\Delta COX}$ cells were treated with increasing concentrations of H_2O_2 [0; 100; 300 µM]. After 6h, release of cytochrome c and activation of caspase 3 was analyzed in cytosolic fractions by Western blot.

Importantly, as already shown in KCN-treated Hela cells, no enhancement of mitochondrial O_2^- generation was detectable in 143B$_{\Delta COX}$ cells, thus excluding that the sensitivity towards H_2O_2 is due to increased basal levels of ROS (Figure 3.8 C). To investigate the role of apoptosis in susceptibility of 143B$_{\Delta COX}$ cells towards oxidative stress, we pre-incubated 143B$_{\Delta COX}$ cells with caspase inhibitors and analyzed cell death after H_2O_2 treatment. In line with our previous data of KCN-treated Hela cells, caspase inhibition by pan-caspase inhibitor zVAD as well as the inhibition of caspase 9 by zIETD completely abolished the enhanced susceptibility of 143B$_{\Delta COX}$ to H_2O_2 treatment (Figure 3.8 D). Accordingly, the increased cell death in 143B$_{\Delta COX}$ towards H_2O_2 was accompanied by an accelerated release of cytochrome c from mitochondria into the cytosol and the subsequent activation of the executioner caspase 3 (Figure 3.8 E).

Genomic ablation of COX10 enhances mitochondrial apoptosis in response to oxidative stress

The murine fibroblast cell line COX10$^{-/-}$ was generated by the transfection of skin fibroblasts of adult mice containing the floxed exon 6 of the assembly factor COX10 with a pCre-Hygro plasmid expressing the P1 Cre recombinase, resulting in the disassembly of the COX holoenzyme and complete knockout of COX (Diaz et al., 2005; Diaz et al., 2006). In line with our previous data obtained in KCN-treated Hela and 143B$_{\Delta COX}$ cell lines, COX10$^{-/-}$ fibroblasts were highly

susceptible to H_2O_2 (Figure 3.9 A), while no alteration in cell death induced by STS could be observed (Figure 3.9 B).

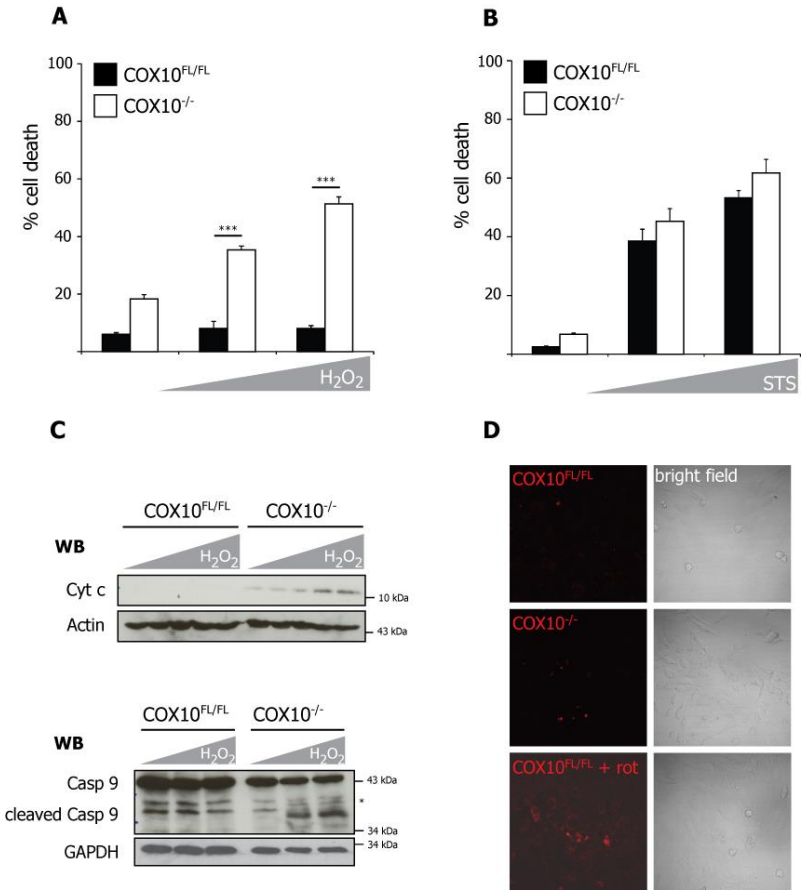

Figure 3.9 | COX10$^{-/-}$ cells display enhanced susceptibility to H_2O_2

(A & B) COX10$^{FL/FL}$ and COX10$^{-/-}$ cells were treated with increasing concentrations of (A) H_2O_2 [0; 100; 200 µM] and (B) STS [0; 50; 100 nM] and cell death was assessed by trypan blue exclusion after 20h (STS) and 24h (H_2O_2), respectively. Error bars represent mean ± SEM (n=4). ***p<0.001

(C) COX10$^{FL/FL}$ and COX10$^{-/-}$ cells were treated with increasing concentrations of H_2O_2 [0; 25; 50; 100; 250 µM]. After 6h, release of cytochrome c from mitochondria was analyzed in cytosolic fractions by Western blot (upper panel). For detection of caspase 9 cleavage, COX10$^{FL/FL}$ and COX10$^{-/-}$ cells were treated with increasing concentrations of H_2O_2 [0; 100; 200 µM] for 16h and total lysates were analyzed by Western blot (lower panel).* = unspecific band

(D) COX10$^{FL/FL}$ and COX10$^{-/-}$ cells were left untreated or treated with rotenone [25 nM] for 3h as indicated and the generation of O_2^- was analyzed with MitoSox^{TM} Red by confocal microscopy.

Consistent with our findings (Figure 3.5 B and 3.8 C) and in line with the previous observation that neuron-specific COX10 knockout does not induce ROS-dependent tissue damage (Diaz et al., 2012), basal levels of O_2^- were not increased in $COX10^{-/-}$ fibroblasts (Figure 3.9 D). Further analyzing the nature of enhanced susceptibility towards oxidative stress revealed that as in KCN-treated Hela cells or $143B_{\Delta COX}$ cybrids, cell death in $COX10^{-/-}$ fibroblasts was a result of an increased mitochondrial apoptosis as evidenced by the accelerated release of cytochrome c and the activation of caspase 9 (Figure 3.9 C).

In conclusion, our data demonstrate that the COX-deficiency in different cell types consistently enhances the mitochondrial apoptotic response specifically towards oxidative stress.

Sphingolipid metabolism is altered upon COX dysfunction

Our data conclusively revealed that COX-deficiency enhances the mitochondrial apoptotic response to oxidative stress. Oxidative stress-mediated activation of caspase has previously been demonstrated to be the result of down-regulation of anti-apoptotic Bcl-2 proteins (Moungjaroen et al. 2006).

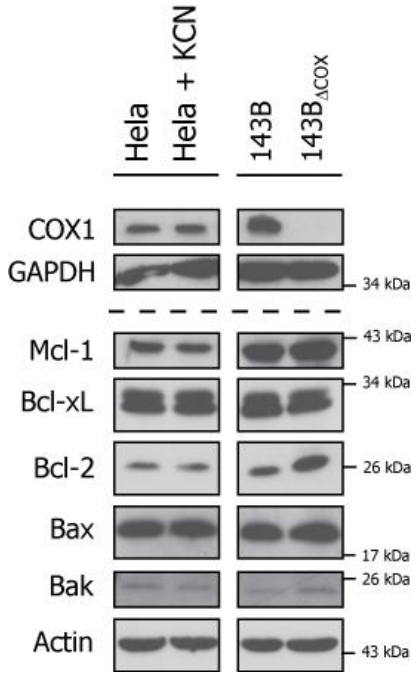

Figure 3.10| Expression patterns of Bcl-2 family members are unaffected by COX dysfunction
Hela cells were left untreated or treated with KCN [1 mM] for 48h. Expression levels of indicated Bcl-2 proteins were analyzed from total cell lysates of Hela, 143B and $143B_{\Delta COX}$ cells by Western blot.

Thus, we hypothesized that an altered expression patterns of the Bcl-2 protein family members in COX-deficient cells is the basis of the increased susceptibility to oxidative stress. However, analysis of the main pro- and anti-apoptotic Bcl-2 protein family members in Hela and 143B cells revealed only a weak increase in the expression of the anti-apoptotic protein Bcl-2 in $143B_{\Delta COX}$ cells, whereas we could not detect further alterations in the expression pattern of other Bcl-2 protein family members (Figure 3.10). Especially, as would have been expected, neither were anti-apoptotic Bcl-2 proteins (Bcl-2, Bcl-xL, Mcl-1) down-, nor pro-apoptotic Bcl-2 proteins (Bax, Bak) up-regulated.

In addition to the Bcl-2 protein family, MOMP can be regulated by modifications of the lipid composition of the outer mitochondrial membrane, and previous observations have repeatedly been demonstrating that the activation of pro-apoptotic Bax and Bak can be controlled by the sphingolipid species ceramide (Siskind et al., 2002; Stiban et al., 2006). Sphingolipids, aside of being crucial components of lipid compartments, have been shown to participate in versatile cellular functions, amongst others, differentiation, proliferation as well as senescence and apoptosis (Hannun & Obeid 2008). To test whether the sphingolipid metabolism and in particular ceramide levels are altered in COX deficient cells, we performed mass spectrometry analysis of whole cell homogenates. Here, we observed that total levels of the majority of the short and long chain ceramides were significantly elevated in all cell lines lacking functional COX (Figure 3.11). In this context, especially the accumulation of short-chain ceramide $C_{16:0}$ in all COX-deficient cell lines is striking, since $C_{16:0}$ ceramides have repeatedly been described to induce apoptosis upon versatile stress conditions and to synergistically act with Bax to induce MOMP (Ganesan et al., 2010; Lee et al., 2011; Aflaki et al., 2012).

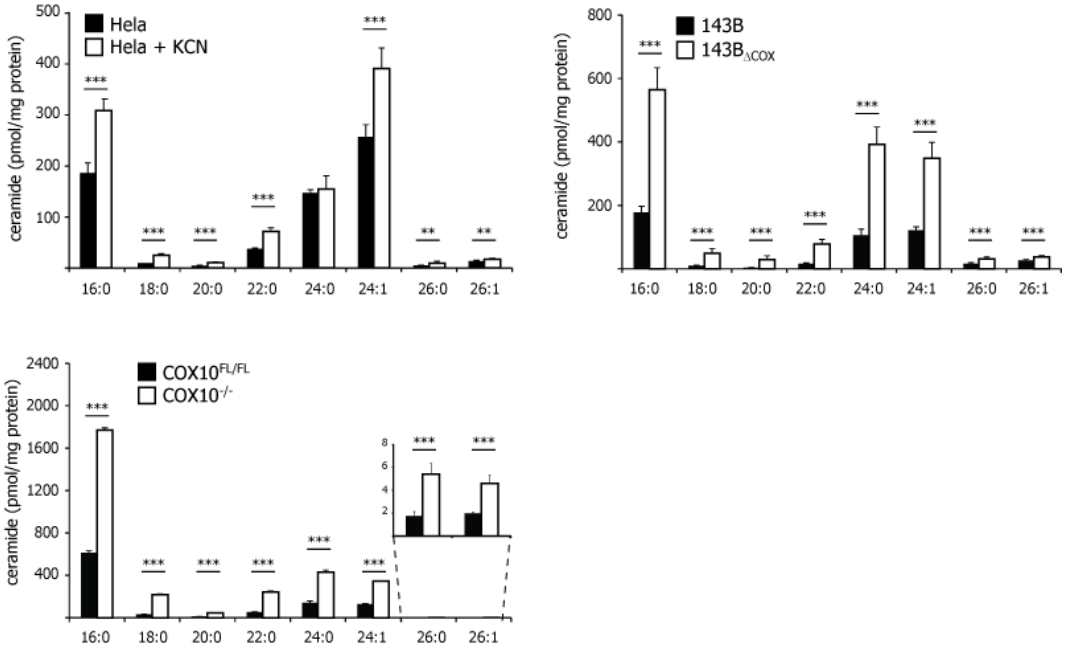

Figure 3.11 | Short and long chain ceramides accumulate in cells with defective COX

Total ceramide content of cells ($2x10^6$) was analyzed by mass spectrometry. Hela cells were left untreated or treated with KCN [1 mM] for 48h. Error bars represent mean ± SD of 2 analytical replicates of 3 biological replicates (Hela and 143B) and mean ± SD of 2 analytical replicates of 2 biological replicates (COX10), respectively. Measurements were performed by Dr. Susanne Brodesser at the Cecad Lipidomics Facility. **p<0.01, ***p<0.001

Representing the center of sphingolipid metabolism, ceramides also act as precursors for the synthesis of sphingomyelins and cerebrosides like glucosylceramide (Mullen et al., 2012). The *de novo* synthesis of sphingolipids is initiated by the conjugation of serine to palmitate and a subsequent reduction step, generating dihydrosphingosine. In mammals, six different ceramide synthases (CerS1-6) synthesize ceramides from dihydrosphingosines or sphingosines in a side-chain specific manner, generating dihydroceramides which are immediately desaturated to ceramides. Among the ceramide synthases, CerS5 and 6 synthesize the pro-apoptotic $C_{16:0}$ and $C_{18:0}$ as well as $C_{14:0}$ ceramides. The redundancy of CerS5 and 6 is still a matter of debate, however CerS6 has been shown to be involved in apoptosis while CerS5, albeit also participating in mediating apoptosis, rather seems to function in ceramide homeostasis (White-Gilbertson et al., 2009; Novgorodov et al., 2011; Hoeferlin et al., 2013). Ceramides can then be reversibly converted into sphingomyelins by sphingomyelin synthases or glycosylated by glucosyl or galactosyl ceramide synthases (Mullen et al. 2012). The accumulation of ceramides can therefore occur for several reasons: 1.) The *de novo* synthesis by ceramide synthases is

enhanced, 2.) ceramide regeneration from sphingomyelins by sphingomyelinases (SMase) at the plasma membrane is increased or 3.) ceramides originate from the so called salvage pathway by reduction of sphingomyelins and glucosylceramides to sphingosine, which can directly act as substrate for ceramide synthases.

To investigate whether the *de novo* synthesis of ceramides is enhanced, we adapted a protocol to analyze ceramide synthesis in viable cells by mass spectrometry (Siskind et al. 2010) and traced the incorporation of exogenous $C_{17:0}$ dihydrosphingosine in control and COX-deficient cells (Figure 3.12).

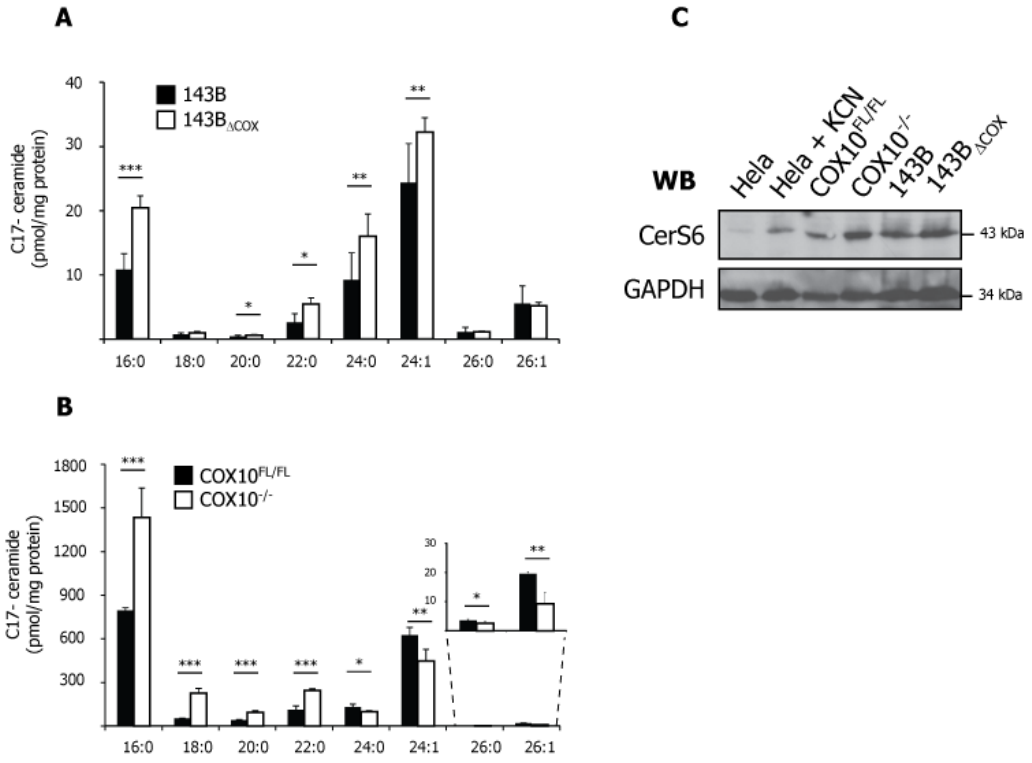

Figure 3.12 | Ceramide synthesis is increased in COX deficient cells

(A & B) Incorporation of $C_{17:0}$ dihydrosphingosine [2 µM] into ceramides after 4h was assessed by mass spectrometry of total cell homogenates of at least $2x10^6$ cells. Hela cells were left untreated or treated with KCN [1 mM] for 48h. Error bars represent mean ± SD of 2 analytical replicates of 4 biological (143B) and 2 biological (COX10) replicates, respectively. Measurements were performed by Dr. Susanne Brodesser at the Cecad Lipidomics Facility. *p<0.05, **p<0.01, ***p<0.001

(C) Representative Western blot detecting expression of CerS6 in Hela cells untreated or treated with KCN [1 mM] for 48h, 143B and 143B$_{\Delta COX}$ and COX10$^{FL/FL}$ and COX10$^{-/-}$ cells.

Dihydrosphingosine is the physiological substrate to which the specific acyl side-chain is attached by corresponding ceramide synthases during *de novo* synthesis of ceramides. Incorporation of $C_{17:0}$ dihydrosphingosine into short chain ceramides was significantly enhanced in ΔCOX cybrids and $COX10^{-/-}$ fibroblasts, indicating that ceramide synthesis is increased. Accordingly, the analysis of the expression level of the responsible CerS for $C_{16:0}$ ceramide revealed an elevated expression of CerS6 in COX deficient cells (Figure 3.12 C).Apoptosis induction by versatile stress inducers including CD95, TRAIL, UV-light or H_2O_2 has been shown to result from increased generation of ceramides by the SMases (Goldkorn et al., 1998; Kashkar et al., 2005; Dumitru & Gulbins, 2006). To test whether modifications in the activity of SMases could be responsible for the observed increase in total ceramide concentrations in COX-deficient cells, we performed SMase activity-assays as described previously (Wiegmann et al., 1994) (Figure 3.13).

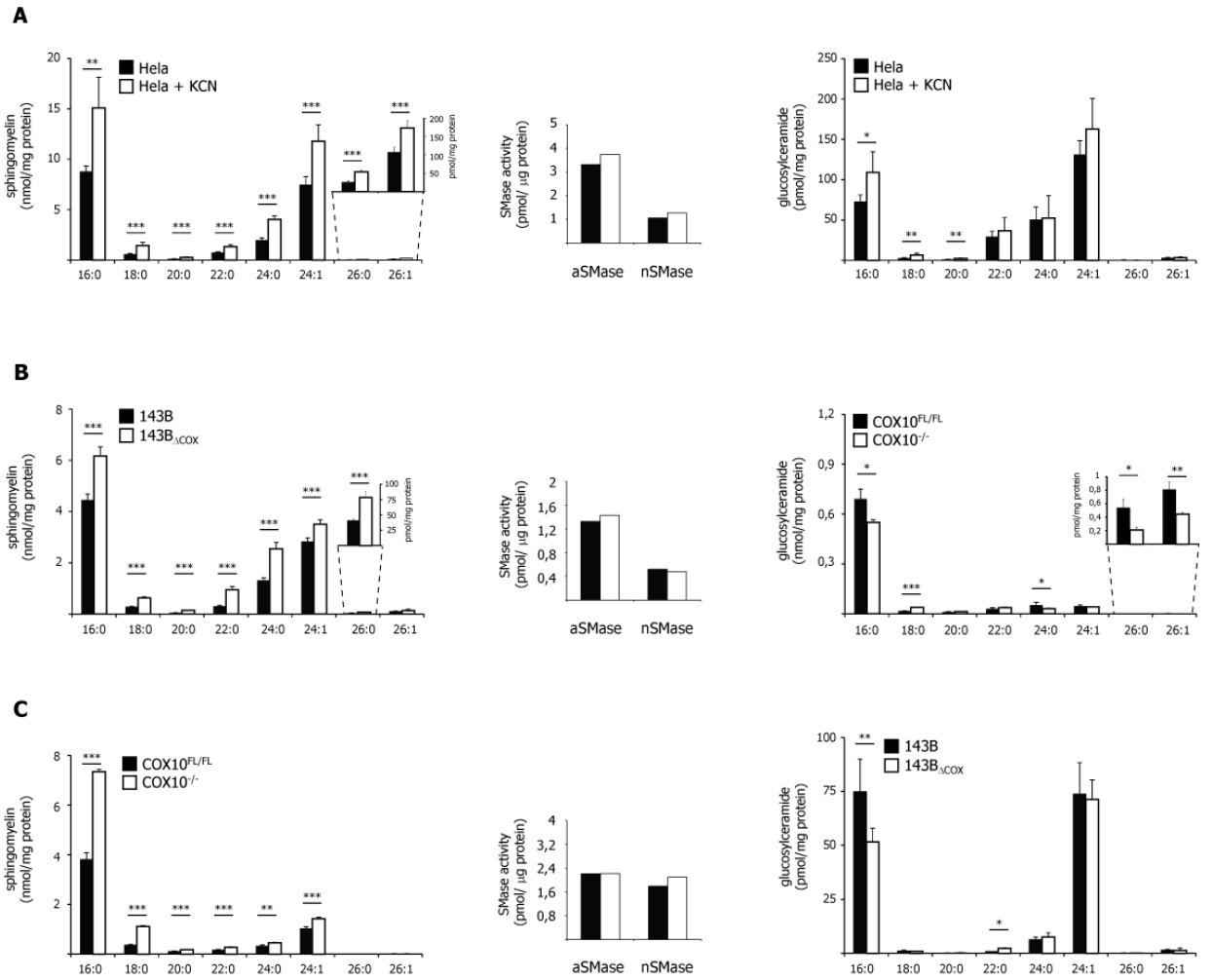

Figure 3.13 | COX dysfunction increases intracellular sphingomyelins and reveals little disturbance on glucosylceramide metabolism

Total sphingomyelin and glucosylceramide concentrations of at least 2x106 cells were analyzed by mass spectrometry by Dr. Susanne Brodesser at the Cecad Lipidomics Facility. Neutral and acid SMase activity was measured from crude cytosolic extracts (nSMase) or total cell lysates (aSMase) of at least $3x10^6$ cells by Katja Krönke-Wiegmann. Hela cells were left untreated or treated with KCN [1 mM] for 48h. Error bars represent mean ± SD of 2 analytical replicates of 3 biological replicates (Hela and 143B) and mean ± SD of 2 analytical replicates of 2 biological replicates (COX10), respectively. **p<0.01, ***p<0.001

We could not observe alterations in the activity of neither acid nor neutral sphingomyelinase in COX-deficient cells compared to controls (Figure 3.13, middle panel) and the increase in total cellular sphingomyelin content indicates that sphingolipid *de novo* synthesis in general is modified (Figure 3.13, left panel).

Furthermore, in addition to *de novo* synthesis or sphingomyelin-breakdown, ceramide may accumulate by the conversion of glucosylceramides, which normally exist in comparable molar amounts within various cell types. However, our analyses of the intracellular levels of glucosylceramides revealed no persistent modifications within the different acyl side-chains, thus it seems unlikely that enhanced glucosylceramide-breakdown is responsible for the elevated cellular ceramide content upon COX dysfunction (Figure 3.13 A-C, right panel).

Taken together, COX dysfunction leads to the accumulation of pro-apoptotic $C_{16:0}$ ceramide as a result of an increased *de novo* ceramide synthesis through elevated expression of CerS6.

Inhibition of ceramide $C_{16:0}$ *de novo* synthesis completely rescues COX dysfunctional cells from ROS induced apoptosis

Having demonstrated that the *de novo* synthesis of ceramide is responsible for the increased mitochondrial apoptosis in response to oxidative stress, we hypothesized that the inhibition of the enzymatic activity of CerS6 should diminish the increased susceptibility to H_2O_2 in COX-deficient cells. Whole ceramide synthase family activity can be inhibited by the mycotoxin fumonisin B1 (FB1), which due to its structural similarity acts as a competitive inhibitor of sphingosine and dihydrosphingosine for the binding site of the enzymes (Wang et al., 1991). Accordingly, pre-treatment of all three COX-deficient cell lines with FB1 significantly reduced cell

death and the release of cytochrome c as evidenced in Hela cells upon treatment with H_2O_2 (Figure 3.14 A and C).

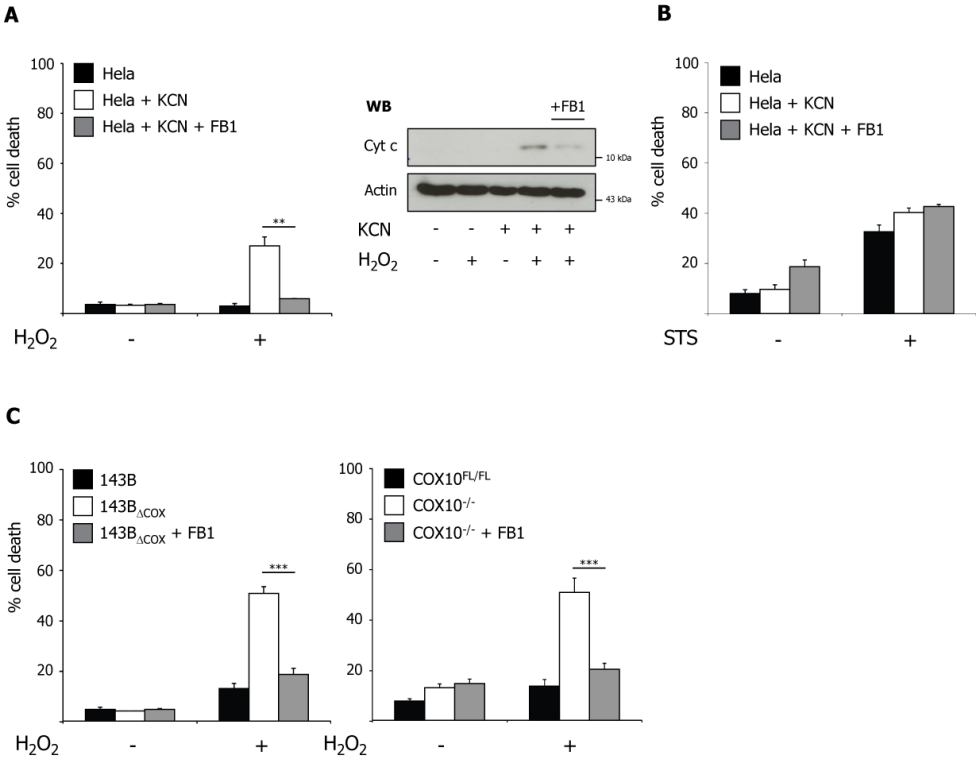

Figure 3.14 | Inhibition of the CerS family by FB1 rescues COX deficient cells from H_2O_2 induced apoptosis

(A & B) Hela cells were treated or left untreated with KCN [1 mM] and FB1 [20 µM]. After 24h cells were treated with H_2O_2 [50 mM] or STS [100nM] and cell death was assessed by trypan blue exclusion after (A) 20h and release of cytochrome c was analyzed in cytosolic extracts after 6h by Western blot (right panel) or (B) 18h.

(C) $143B_{\Delta COX}$ cells were left untreated or treated with FB1 [30 µM]. After 24h, cells were treated with H_2O_2 [250 µM] and cell death was assessed by trypan blue exclusion after 16h (left panel). $COX10^{-/-}$ cells were left untreated or treated with FB1 [50 µM]. After 24h, cells were treated with H_2O_2 [100 µM] and cell death was assessed by trypan blue exclusion after 20h (right panel). **p<0.01, ***p<0.001

Additionally, STS-induced apoptosis was unaffected by the inhibition of ceramide synthases, further underlining the specific role of ceramides in conducting COX-deficiency induced apoptosis to oxidative stress (Figure 3.14 B). More specifically, an siRNA mediated specific

knockdown of CerS6 resulted in a reduction of cell death in all COX-deficient cell lines (Figure 3.15 A, C and E), and knockdown of CerS6 was sufficient to block the release of cytochrome c and activation of caspase 9, highlighting the central role of CerS6 in COX-deficiency mediated susceptibility to oxidative stress (Figure 3.15 B and D).

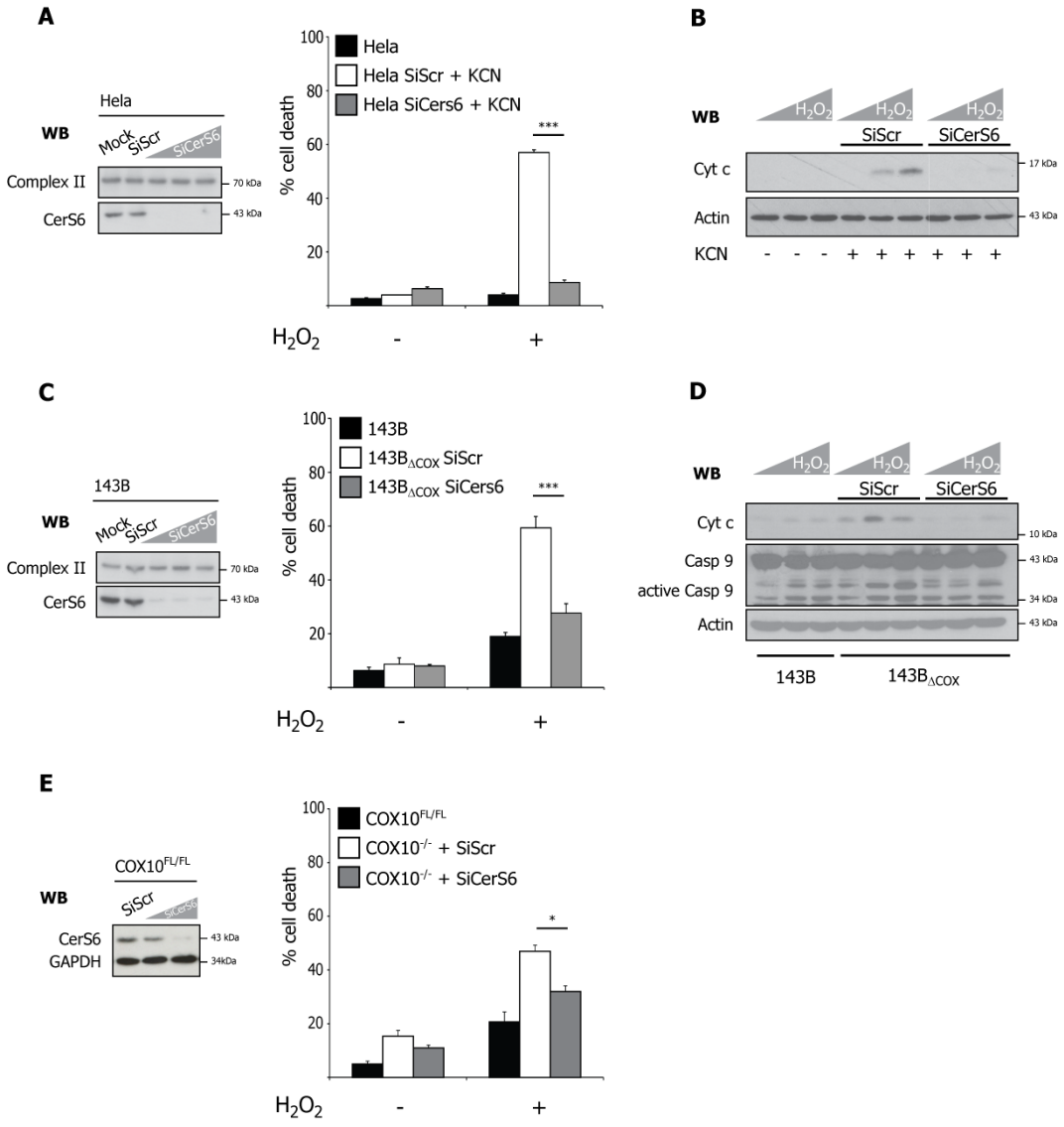

Figure 3.15 | siRNA mediated knockdown of CerS6 abrogates H_2O_2 induced apoptosis in COX deficient cells

(A) Hela cells were transfected with siScr [25 nM] or increasing concentrations of CerS6 specific siRNA [25, 50, 75 nM] and knockdown of CerS6 was assessed after 72h by Western blot (left panel). Hela cells were either transfected with siScr [25nM] or siCerS6 [50 nM]; after 24h, cells were left untreated or treated with KCN [1 mM]. After 48h, cells were treated with H_2O_2 [50 µM] and cell death was assessed by trypan blue exclusion after 20h (right panel).

(B) Hela cells were treated as in (A). After 48h cells were treated with increasing concentrations of H_2O_2 [0, 50, 150 µM] and release of cytochrome c was analyzed in cytosolic fractions after 6h by Western blot. For detection of caspase 9 cleavage, total cell lysates were analyzed after 12h by Western blot
(C) 143B cells were treated with siScr and siCerS6 as in (A) and knockdown of CerS6 was assessed after 72h by Western blot (left panel). 143B cells were either transfected with siScr [25nM] or siCerS6 [50 nM]; after 48h cells were treated with H_2O_2 [150 µM] and cell death was assessed by trypan blue exclusion after 20h (right panel).
(D) 143B cells were treated with siScr and siCerS6 as in (A). After 48h cells were treated with increasing concentrations of H_2O_2 [0, 150, 300 µM] and release of cytochrome c and cleavage of caspase 9 was analyzed in cytosolic fractions after 6h by Western blot
(E) $COX10^{FL/FL}$ cells were transfected with siScr [25 nM] or siCerS6 [25, 75 nM] and knockdown of CerS6 was assessed after 48h by Western blot (left panel). COX10 cells were either transfected with siScr [25 nM] or siCerS6 [75 nM]; after 24h cells were treated with H_2O_2 [300 µM] and cell death was assessed by trypan blue exclusion after 24h (right panel). *$p<0.05$, ***$p<0.001$

Based on these findings, we assumed that the overexpression of CerS6 alone should confer susceptibility to H_2O_2. Therefore, Hela cells were transfected with DNA constructs encoding either GFP-tagged CerS6, the enzymatic inactive mutant of $CerS6_{R131A}$, CerS3 (generating C_{24} and C_{26}-ceramides) or GFP alone and subsequently subjected to H_2O_2 (Figure 3.16). Only overexpression of CerS6 resulted in activation of Bax and the release of cytochrome c (Figure 3.16, second row), while neither the overexpression of the enzymatic inactive CerS6 mutant (fifth row) nor CerS3 induced apoptosis (fourth row).

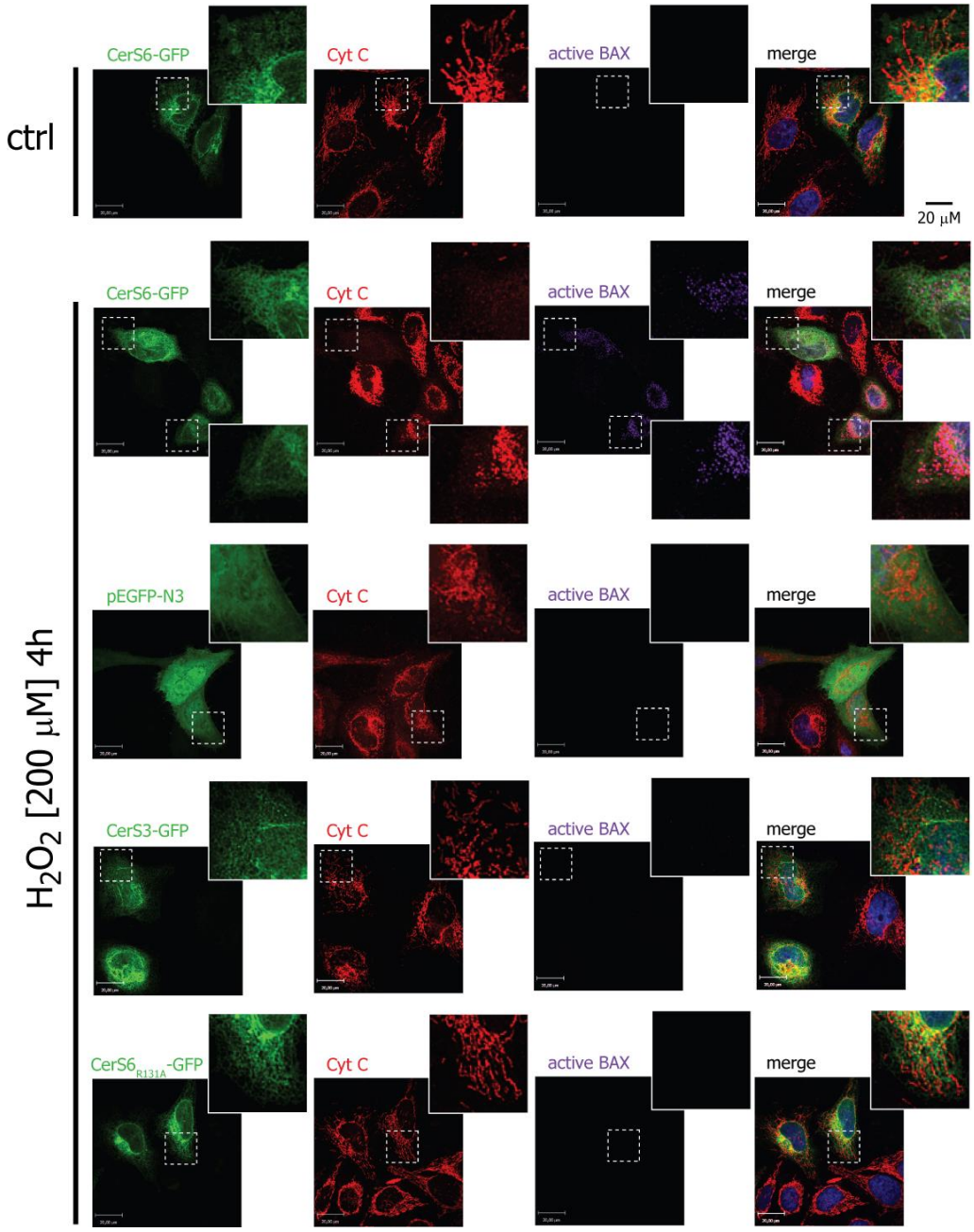

Figure 3.16 | Overexpression of CerS6, but not CerS3 or inactive CerS6, induces apoptosis in Hela cells treated with H_2O_2

Hela cells were transfected with the indicated CerS-GFP constructs or empty vector. After 24h, cells were subjected to 200 µM H_2O_2 for 4h. Cells were fixed and cytochrome c and active Bax were visualized by appropriate antibody staining. Images were taken by Saskia Günther.

Together, these data identify CerS6 as the key mediator of the COX-deficiency induced accumulation of pro-apoptotic $C_{16:0}$ ceramide.

Generation of liver-specific COX10 knockout mice on CerS6 knockout and wild type background

Having shown the importance of the COX-deficiency induced accumulation of ceramides *in vitro*, we wanted to investigate the physiological relevance of our findings within a previously described mouse model. The liver specific COX knockout mice from the group of Carlos Moraes developed severe and fatal hepatopathies (Diaz et al., 2008), while hemizygous Cre expression revealed a patchy distribution of COX-deficient and simultaneously apoptotic hepatocytes. Interestingly, the liver in these animals fully recovered during lifetime, representing effective liver regeneration driven by fully respiring hepatocytes. Having demonstrated that COX-deficiency induced accumulation of $C_{16:0}$ ceramide sensitizes towards H_2O_2-induced apoptosis *in vitro*, we hypothesized that $C_{16:0}$ ceramide physiologically serves to mediate apoptosis in COX-deficient hepatocytes and therefore contributes to liver regeneration *in vivo*. These findings prompted us to generate liver specific COX knockout mice on a Lass6 (*longevity assurance gene*, the gene coding for CerS6) deficient background. CerS6 knockout mice were generated by the Group of Martin Krönke and Jens Brüning using the Cre-lox recombination technology. These mice display no obvious phenotype and develop normally (unpublished results).

To date, we did not succeed in generating mice homozygous for the floxed COX allele and AFP-Cre positive on a homozygous CerS6-kbockout background, as exemplified by two independent breedings in Figure 3.17. From our statistical analysis, one may conclude that the liver-specific knockout of COX is embryonic lethal. However, we also did not receive Cre-positive offspring with homozygous floxed COX alleles on heterozygous (Figure 3.17) or wild type CerS6 background (not shown).

In summary, despite ongoing breeding, until now we have to conclude that the presumed embryonic lethality cannot be attributed to deficiencies in CerS6 expression alone.

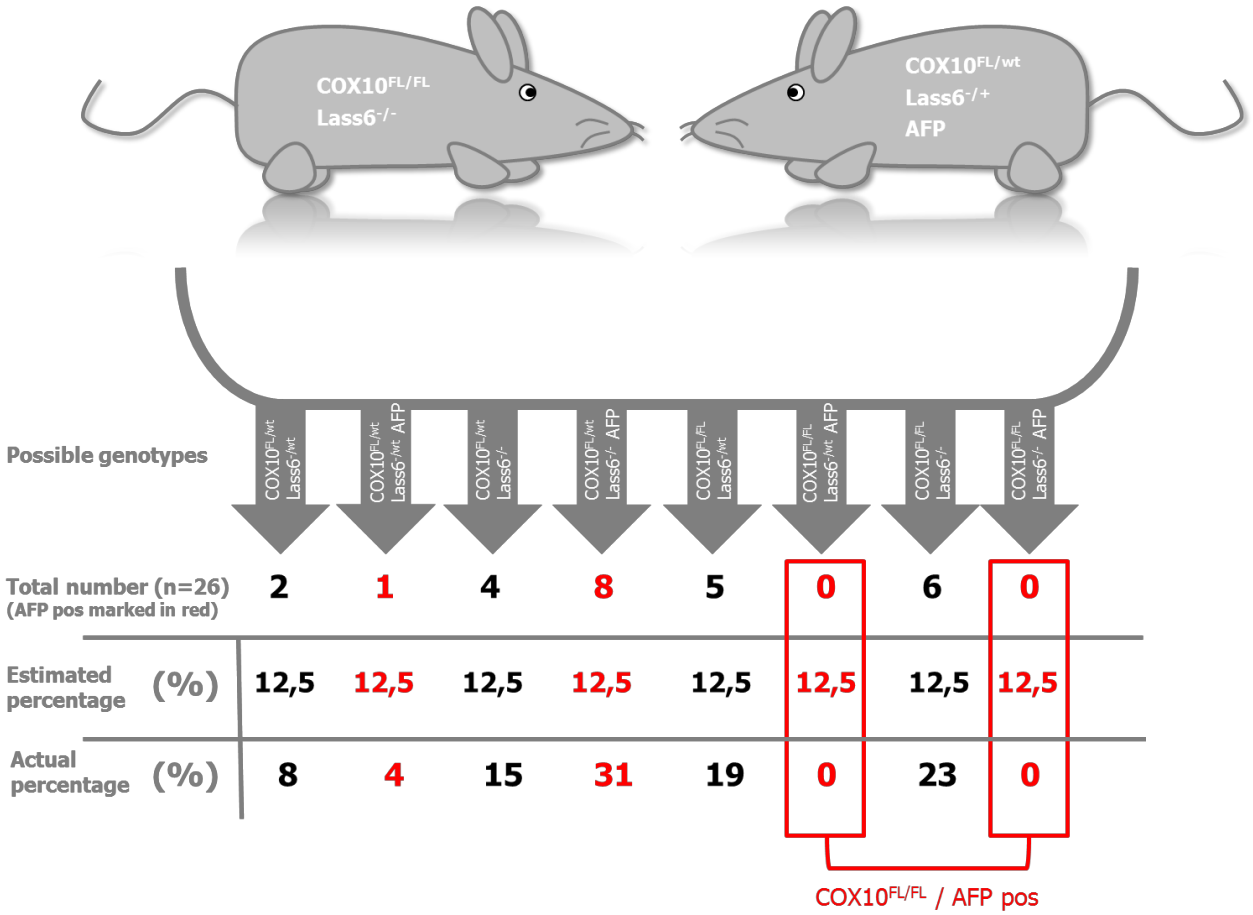

Figure 3.17 | Breeding of floxed COX10/Lass6$^{-/-}$ mice with floxed COX10/Lass6$^{-/wt}$ AFP(+) mice did not generate mice with homozygous knockout of COX

Initial breeding of AFP-positive mice with COX10$^{FL/FL}$Lass6$^{-/-}$ mice generated mixed offspring of COX10$^{FL/wt}$Lass6$^{-/wt}$ mice with an AFP-negative to positive ratio of 5.3:4.7. Backcrossing of AFP-positive mice with COX10$^{FL/FL}$Lass6$^{-/-}$ mice did not result in offspring with homozygous floxed COX10 allele, reflected by a shift of the AFP negative to positive ratio of 6.5:3.5.

Discussion

Since the first discovery of diseases-causing mutations of nuclear (Bourgeron et al., 1995) and mitochondrial DNA (Holt et al., 1988; Wallace et al., 1988) encoded oxidative phosphorylation (OXPHOS) proteins, the role of mitochondrial respiratory chain defects in the onset of degenerative diseases has been confirmed by tremendous research efforts (Ylikallio & Suomalainen 2012). In particular, strong correlations between the decline of mitochondrial respiratory capacity and the incidence of cellular death and tissue degeneration have been extensively described (Breuer et al. 2013). However, our knowledge about the nature of the cellular death process caused by defective mitochondrial respiration remains incomplete.

In the present work we demonstrate a selective susceptibility of cells with deficient cytochrome c oxidase (COX), the terminal complex of the mitochondrial respiratory chain, towards hydrogen peroxide (H_2O_2) treatment. By contrast, the inhibition of all other OXPHOS complexes does not induce H_2O_2 sensitivity. In particular, we observe a significant increase in mitochondrial apoptotic signaling in response to H_2O_2 in COX-deficient cells. Mechanistically we show that COX-dysfunction facilitates apoptosis by the accumulation of the pro-apoptotic sphingolipid species $C_{16:0}$ ceramide. The accumulation of ceramides in COX-dysfunctional cells is the result of enhanced expression of the respective ceramide synthase (CerS) 6 and increased *de novo* synthesis. The inhibition as well as the knockdown of CerS6 abrogates the COX-dysfunction induced susceptibility to H_2O_2 underscoring the central role of CerS6 in this process.

Inhibition of COX reveals selective susceptibility to oxidative stress

How distinct defective respiratory chain complexes contribute towards the induction of cell death is currently unknown. Nonetheless the cytotoxic role of reactive oxygen species (ROS) in degenerative diseases and aging tissues (Lin & Beal, 2006) is indisputable. But even though the nature of ROS-induced cell death has been subject to long-timed debates, whether and how oxidative damage induces cell death in degenerative states is not clear. Our present study demonstrates that the chemical inhibition of COX but none of the other OXPHOS complexes selectively enhances the susceptibility to oxidative stress by H_2O_2 (Figure 3.2), but not to staurosporine (STS). This initial observation was further confirmed using COX-deficient cybrids and knockout fibroblast (Figure 3.8 and 3.9).

COX-deficiency has been linked to various degenerative diseases affecting single tissues (e.g. encephalopathy, myopathy, hepatopathy) or multiple organs (MELAS, LS). *In vitro* and *in vivo* analyses support the notion that defects in COX promote cell death and fatal tissue demise (Diaz, 2010). Moreover, COX-deficiency has been shown to results in enhanced apoptotic cell death (Agostino et al., 2003; Baden et al., 2007; Diaz et al., 2008) and in patients with COX-deficiency, oxidative stress was accompanied by increased apoptosis in myofibers (Di Giovanni et al. 2001). However, the underlying molecular mechanisms driving COX-deficiency induced apoptosis to oxidative stress remains unclear. In this context, our data clearly demonstrate that H_2O_2 induces apoptosis in COX-deficient cells by initiating the activation of Bax, resulting in the permeabilization of the outer mitochondrial membrane (MOMP) and subsequent release of cytochrome c into the cytosol and activation of caspases (Figure 3.4, 3.8 and 3.9). MOMP is tightly regulated by pro- and anti-apoptotic members of the Bcl-2 family (Youle & Strasser 2008). Remarkably, the expression profiles of pro- and anti-apoptotic molecules have been demonstrated to be altered as a cause of retrograde signaling of defective mitochondria to the nucleus (Chandra et al., 2002) and mtDNA depletion-induced resistance to apoptosis is suggested to result from the altered expression of Bcl-2 proteins, thus shifting the balance towards anti-apoptotic Bcl-2 and Bcl-xL (Biswas et al., 2005). These findings might provide a possible explanation of how OXPHOS dysfunction affects the apoptotic fate of cells. By contrast, our present study demonstrates that neither the inhibition of COX by KCN nor COX-deficient cybrids revealed altered expression profiles of the major anti- and pro-apoptotic Bcl-2 proteins that could explain the observed enhanced apoptosis (Figure 3.10). Thus, the observed selective sensitivity to apoptosis upon H_2O_2 treatment is unlikely to be a consequence of misbalanced apoptosis sensing by the Bcl-2 family. It rather seems that in contrast to severe depletions of mtDNA resulting in a global loss of mitochondrial-encoded proteins, the distinct deficiency of COX does not interfere with the cellular orchestration of Bcl-2 proteins. However, Bcl-2 proteins are not only transcriptionally, but also post-translationally regulated, and modifications of the phosphorylation status of different serine-residues of e.g. Bcl-2, Mcl-1 or Bax have been shown to be essential for the induction or inhibition of apoptosis (Ito et al., 1997; Domina et al., 2004; Gardai et al., 2004). Thus, COX-deficiency may impact on the post-translational regulation of Bcl-2 proteins. Further analyses of the post-translational modification of Bcl-2 proteins in cells harboring dysfunctional COX could substantially contribute to our understanding of the role of Bcl-2 proteins in COX-deficiency derived degenerative states.

Accumulation of ceramides sensitizes COX-deficient cells towards oxidative stress-induced apoptosis

Our observations show that COX-deficiency induced *de novo* generation of ceramides is the key component of the apoptotic cell death upon oxidative stress (Figure 3.14-3.16). In particular, we show that the inhibition of the synthesis of pro-apoptotic $C_{16:0}$ ceramide is sufficient to prevent apoptosis upon oxidative stress, but upon treatment with STS (Figure 3.14). Of note, we only observed a relatively small increase of total ceramide $C_{16:0}$ in Hela cells treated with COX-inhibitor KCN (~1.65 fold) compared to total $C_{16:0}$ ceramide increase in COX cybrids (~3.18 fold) and knockout fibroblasts (~2.9 fold) (Figure 3.11). This might reflect the incomplete inhibition of COX as indicated by residual rates of respiration revealing approx. 22% of residual O_2 consumption (Figure 3.1), while in contrast, respiration was shown to be completely absent in ΔCOX cybrids (Kwong et al., 2007) and $COX10^{-/-}$ fibroblasts (Diaz et al., 2006).

Ceramides were shown to have the immanent capability of inducing transmembrane pores in cell free phospholipid bilayers (Siskind & Colombini, 2000) and in isolated mitochondria, capable of triggering the release of proteins up to 60kDa in size (Siskind et al., 2002). Accordingly, the release of pro-apoptotic intermembrane proteins like cytochrome c (14 kDa) or second mitochondrial derived activator of caspases (SMAC, 21 kDa) is assumed to result from ceramide pore formation on the outer mitochondrial membrane. However, the majority of experiments initially performed on cell free membrane systems and on isolated mitochondria relied on the use of the synthetic and water-soluble ceramide-analogs ceramide C_2 or C_6 ceramide. These synthetic analogs differ considerably in their biophysical properties from naturally occurring ceramides and are hence inappropriate to reflect physiological components of biological membranes.

In this regard, our data demonstrate that the release of cytochrome c is critically dependent on the activation of Bax and Bak in COX-deficient Hela cells (Figure 3.6 and 3.16), suggesting further involvement of pro-apoptotic Bcl-2 proteins in conducting $C_{16:0}$ ceramide induced cell death. Within the current model, the release of mitochondrial proteins during apoptosis is the consequence of conformational change and subsequent activation of Bax and Bak (Youle & Strasser 2008). In support of our data, Bax and $C_{16:0}$ ceramide have been demonstrated to act synergistically in conducting the release of mitochondrial intermembrane space proteins (Ganesan et al. 2010). Ganesan et al. demonstrated that in the presence of $C_{16:0}$ ceramide, the induction of MOMP in isolated rat liver mitochondria is enhanced upon incubation with cleaved

human Bid (tBid) and recombinant human Bax. The authors propose a model in which ceramide-induced membrane pores are distorted by membrane bound active Bax oligomers, enlarging the pore by insertion of accessory $C_{16:0}$ ceramides until the size of its curvature matches that of active Bax. In addition, our findings are supported by previous work of our own lab demonstrating that Bax activation and the release of mitochondrial intermembrane proteins upon UV-C stress (Kashkar et al., 2005) was dependent on the availability of $C_{16:0}$ ceramides.

In general, Bax and Bak are described to have redundant functions in apoptotic signaling, however a MOMP-independent function of Bak has been suggested recently (Beverly et al. 2013). In particular, it has been demonstrated that Bak is an indispensable activator for the immediate generation of $C_{16:0}$ ceramides upon stress induction (Siskind et al., 2010). The authors demonstrated that Bak knockout fibroblast displayed a significant decrease in ceramide accumulation and ceramide synthase activity upon UV-C stress, while the ceramide increase in Bax-deficient cells was comparable to wild type cells. In KCN-treated single knockout fibroblasts of Bax or Bak, we observed indistinguishable resistance towards H_2O_2 treatment (Figure 3.6), suggesting that the contribution of Bak to $C_{16:0}$ ceramides triggered apoptosis towards oxidative stress in COX-deficient cells is presumably restricted to its known pro-apoptotic features. In line, in COX-deficient cells ceramide accumulation preceded cell death and sensitized cells to oxidative stress induced apoptosis, whereas in the above-mentioned work by Siskind et al. and Beverly et al., ceramide accumulation was the consequence of apoptosis induction. Thus different mechanisms might control apoptotic induced and mitochondrial dysfunction-driven ceramide synthesis.

Bax/Bak-mediated MOMP is antagonized by anti-apoptotic Bcl-2 proteins (Tait & Green 2010). Congruently, we demonstrate that Bcl-2 overexpression completely inhibited MOMP in response to oxidative stress in COX-deficient Hela cells (Figure 3.7). However, as already noted before, anti-apoptotic Bcl-2 family members have repeatedly been shown to administrate additional functions beyond the inhibition of MOMP. In a work by Sawada and colleagues, transient or stable overexpression of Bcl-2 and Bcl-xL rescued rat glioma or human glioblastoma cells from etoposide, cisplatin or TNF-α induced apoptosis by inhibiting ceramide synthesis of aSMase (Sawada et al., 2000), presenting an alternative way of apoptosis inhibition by Bcl-2 proteins. However, as already mentioned above, we did not observe changes in the expression of neither Bcl-2 nor Bcl-xL in COX-deficient cells (Figure 3.10). However, Ruvolo et al. have shown that apoptosis by exogenous ceramides-analogs is accompanied by the activation of a mitochondrial

phosphatase of the PP2A family which presumably results in the inhibition of Bcl-2 by dephosphorylation of serine 70 (Ruvolo et al., 1999). Vice versa, Kawatani and coworkers have demonstrated that transmembrane domain-deleted Bcl-2 is still sufficient to inhibit cytochrome c release, but failed to reduce ceramide synthesis (Kawatani et al., 2003). Because Bcl-2 is also localized to the endoplasmic reticulum (ER) (Lithgow et al., 1994), these findings suggest that even though Bcl-2 expression levels are unaltered in COX-deficient cells, Bcl-2 proteins could be involved in the regulation of ceramide synthesis at the ER.

Ceramide Synthase 6 is the key mediator of oxidative stress-induced apoptosis in COX-deficiency

The synthesis of $C_{16:0}$ ceramide is exclusively and redundantly performed by CerS5 and 6, the only CerSs sharing acyl side-chain preference. It appears that both CerS are selectively important under specific physiological conditions, yet their individual contribution towards cell death remains inconsistent and seems to be dependent on the type of stress (Mullen et al., 2012). Here we demonstrate that inhibition of the whole CerS-family is sufficient to selectively reduce susceptibility to oxidative stress in COX-deficient cells (Figure 3.14). Moreover, we provide strong evidence that CerS6 is responsible for the accelerated apoptosis by demonstrating that knockdown rescued COX-deficient and overexpression primed normal respiring cells to oxidative stress (Figure 3.15 and 3.16). Taken together, we here identify a so far unknown role of *de novo* $C_{16:0}$ ceramide synthesis by CerS6 in initiating oxidative stress induced apoptosis in COX-deficient cells.

The observation that the inhibition or absence of COX activity has a direct impact on the *de novo* synthesis of $C_{16:0}$ ceramides which then in turn results in enhanced apoptotic signaling in response to oxidative stress (Figure 3.11-16) raises the question how the dysfunction of an inner mitochondrial membrane protein complex can influence an ER/MAM-residing enzyme. So far only little research has been performed in this regard. However a couple of publications highlighted that $C_{16:0}$ ceramide could actively block COX-activity (Di Paola et al., 2000; Zigdon et al., 2013), indicating that infiltration of ceramides is not merely restricted to the outer membrane, but might also intrude into the inner mitochondrial membrane. Indeed, ceramide incorporation into the inner mitochondrial membrane could be demonstrated (Ardail et al. 2001) and ceramides, like cardiolipin, might be able to modify the activity of respiratory chain

complexes by protein-lipid interactions. Vice versa, contact sites between the outer and inner mitochondrial membrane by the mitochondrial contact site (MICOS) complex localized to cristae junctions has been shown to be critical for accurate mitochondrial function and biogenesis (Harner et al. 2011). Though no respiratory chain complexes could be located to MICOS under physiological conditions, this observation theoretically enables the possibility that other large protein complexes, like respiratory chain complexes, might associate to the outer membrane of dysfunctional mitochondria. Strikingly, COX has been described to be associated with porins in the outer mitochondrial membrane (La Piana et al., 2005) and COX and $C_{16:0}$ ceramid were shown to create contact sites at the outer mitochondrial membrane (Gorgoglione et al. 2010).

Accumulation of total $C_{16:0}$ ceramide in COX-deficient cells could be attributed to increased expression of CerS6 (Figure 3.11), indicating that COX-deficiency is sensed by a yet unknown mechanism(s) resulting in the up-regulation of CerS6. Ceramide accumulation by genotoxic stress or γ-irradiation has initially been revealed to be controlled in a p53-dependent manner (Dbaibo et al. 1998) and more recently, p53 was identified to directly induce *de novo* ceramide synthesis by transcriptionally up-regulating CerS5 in leukemia cells upon y-irradiation (Panjarian et al. 2008). Accordingly, CerS6 has lately been shown to be a transcriptional target of p53 upon folate withdrawal, resulting in increased levels of CerS6 and apoptosis (Hoeferlin et al., 2013). Additionally, the activity of p53 itself has been shown to be modified by distinct mitochondrial respiratory chain defects (Compton et al. 2011), and p53 is assumed to be responsible for the metabolic switch of respiration to enhanced glycolysis in cancer cells by the regulated expression of *synthesis of cytochrome c oxidase* (SCO2) (Matoba et al. 2006; Wanka et al. 2012). Though the role of p53 in regulating respiratory chain activity is complex and solid data concerning its function towards defective mitochondrial respiration is scarce, it seems possible that COX-deficiency induces the up-regulation of CerS6 by p53 to efficiently sense malfunctioned cells to apoptosis.

Remarkably, CerS6 has been readily described as a pro-apoptotic protein and is assumed to be involved in the induction of mitochondrial apoptosis (White-Gilbertson et al., 2009; Novgorodov et al., 2011). CerS6, like all ceramide synthases, has been shown to be localized to the ER (Venkataraman et al., 2002; Riebeling et al., 2003; Mizutani et al., 2005; Laviad et al., 2008) and compelling unpublished data by our own group analyzing the subcellular localization of all CerS strongly support previous findings. However, the mechanism of how CerS6 initiates the release of mitochondrial intermembrane proteins remains elusive. Like many enzymes of the

lipid metabolism, CerS are hydrophobic membrane proteins and ceramides are likewise hydrophobic, neutral molecules restricted to their compartments of formation. Trafficking of ceramides from the ER to the Golgi network is executed by ceramide transfer protein (CERT) in a non-vesicular manner, and membrane contact sites of both compartments are assumed to contribute to efficient ceramide translocation (Hanada et al., 2007). So far, there is no evidence for carrier protein shuttling of ceramides from ER to mitochondria. However, ER and mitochondria are not only connected by physiological means, but are also in close spatial interaction (de Brito & Scorrano 2008; Friedman et al. 2011; Csordás et al. 2006), presumably close enough to allow direct translocation of ceramides from the ER-membrane to the mitochondrial outer membrane. Strikingly, ceramides were shown to readily flip between adjacent membrane compartments (López-Montero et al. 2005) and CerS5 and 6 were found in mitochondria associated membranes (MAMs). MAMs are ER-derived membrane compartments in close proximity to mitochondria and have been shown to harbor fundamental components of the lipid metabolism (Vance, 1990; Raturi & Simmen, 2013). Further, the close proximity is assumed to be crucial for the induction of apoptosis by $C_{16:0}$ ceramide, and it seems possible that ER and mitochondria in close juxtaposition facilitate a surrounding in which hydrophobic lipids are shared by both membrane compartments. Accordingly, it has been demonstrated that ceramides are translocated from MAMs to mitochondria by vesicular transport (Stiban et al., 2008).

Physiological relevance

Apoptosis as the physiological cell death is an essential component of cellular homeostasis and tissue regeneration (Bergmann & Steller 2010). While reduced apoptosis has been shown to be a prerequisite for the formation of cancer (Hanahan & Weinberg 2011), excessive apoptosis is assumed to precipitate degenerative states and is implicated in aging and aging-associated diseases (Dean, 2008; Breuer et al., 2013). However, it remains controversial whether excessive apoptosis is merely detrimental or beneficial in an aging tissue progressively exposed to stress conditions. Accordingly, potential benefits of inhibiting apoptosis has been anticipated in degenerative diseases including Alzheimer's disease (Dickson 2004; Rohn 2010).

Based on our incomplete knowledge about the mode of cellular demise within an aging tissue and the lack of molecular insights about the crosstalk of degenerative alterations and the cellular death machinery, research has been hampered to comprehensively prove the role of cell

death in degenerative and aging-associated diseases as well as its regulation in tissue regeneration. In liver, alteration of OXPHOS leads to mitochondrial hepatopathy, which rapidly progresses to liver failure in some patients. Alternatively, liver pathology may spontaneously reverse without manifestation of severe disease. Similarly, in the afore-mentioned mitochondrial hepatopathy mouse model created by liver-specific ablation of COX10 gene, some mice showed severe COX-deficiency and early liver pathology, but had a complete reversion of all pathological phenotypes resulting in a normal mouse life span (Diaz et al. 2008). The continuous replacement of damaged hepatocytes and the lack of collateral liver damage upon COX-dysfunction indicate the involvement of a controlled hepatocytic demise, which is decisive for the coordinated liver regeneration. However, the role and the control of cellular death machineries during the course of the pathogenesis of mitochondrial hepatopathy have not been elucidated. The present study shows for the first time how mechanistically apoptosis is triggered upon COX-dysfunction. Further investigations by employing $CerS6^{-/-}$ or $Bcl2^{tg}$ (blocking mitochondrial apoptosis) mice will substantially help us to understand the role of apoptosis in an aging tissue. One striking hypothesis would be to induce apoptosis in order to efficiently eliminate damaged cells in an aging tissue. This would enable the tissue to regenerate and to replace the apoptotic cells. Especially in mtDNA-derived COX-disorders an efficient removal of deficient cells with high loads of heteroplasmic mitochondria is crucial to prevent the onset of degenerative states, and sensing of COX-deficient cells by $C_{16:0}$ ceramide accumulation could be one possible mode of action. This hypothesis is supported by clinical data: Childhood-onset of COX-deficiency derived degeneration disorders like encephalopathy, myopathy, hepatopathy or combined encephalomyopathy and encephalohepatopathy are usually severe and fatal at early age. However, case reports have repeatedly demonstrated that in some patients, affected tissues almost fully recovered within the very first years of age (DiMauro et al., 1983; Nonaka et al., 1988; Salo et al., 1992; Zeharia et al., 2009; Schara et al., 2011) and recent work revealed that COX levels fully recovered as evidenced by histochemical staining and protein expression (Horvath et al. 2009).

In line with our results concerning the pro-apoptotic role of CerS6 in an aging tissue, accumulating recent evidence suggest that silencing CerS6 in cancer promotes drug-resistance in a variety of cancer entities including colon, liver, pancreatic and ovarian cancer (Walker et al. 2009; White-Gilbertson et al. 2009). Together with our findings these observations indicate the therapeutic role of CerS in cancer as a regulatory node of apoptosis.

In conclusion, our data substantiate previous findings and provide further mechanistic insights into how enhanced cell death could contribute to the demise of COX-deficient cells. Our data strongly imply that further analyses of the exact molecular crosstalk between COX and CerS6 might unravel essential aspects of efficient tissue regeneration and could additionally facilitate the introduction of potential therapies of COX-deficiency disorders (Figure 4.1).

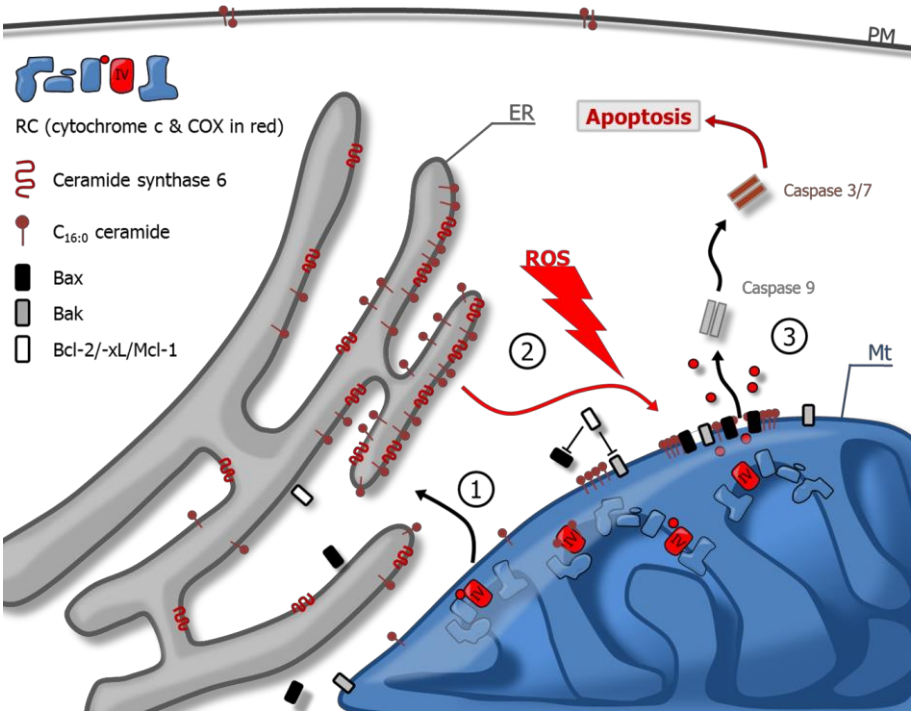

Figure 4.1 | Proposed model of COX-deficiency induced apoptosis towards oxidative stress
COX-deficiency leads by a yet unknown mechanism to enhanced expression of CerS6 and accumulation of intracellular $C_{16:0}$ ceramide, presumably at the ER (1). Upon oxidative stress, $C_{16:0}$ ceramide translocates to mitochondria and induces Bax and Bak dependent permeabilization of the outer mitochondrial membrane (2). Release of cytochrome c from the mitochondrial intermembrane space induces the activation of initiator-caspase 9 and downstream executioner-caspases, finally resulting in apoptosis of the COX-deficient cell (3).Mt, mitochondria; PM, plasma membrane; RC, respiratory chain.

References

Aflaki, E. et al., 2012. C16 ceramide is crucial for triacylglycerol-induced apoptosis in macrophages. *Cell death & disease*, 3, p.e280.

Agostino, A. et al., 2003. Constitutive knockout of Surf1 is associated with high embryonic lethality, mitochondrial disease and cytochrome c oxidase deficiency in mice. *Human Molecular Genetics*, 12(4), pp.399–413.

Anderson, A. et al., 1981. Sequence and organization of the human mitochondrial genome. *Nature*, 290, pp.457–465.

Ardail, D. et al., 2001. Occurrence of ceramides and neutral glycolipids with unusual long-chain base composition in puri ¢ ed rat liver mitochondria. *FEBS letters*, 488, pp.160–164.

Auré, K. et al., 2006. Apoptosis in mitochondrial myopathies is linked to mitochondrial proliferation. *Brain : a journal of neurology*, 129, pp.1249–59.

Baden, K.N. et al., 2007. Early developmental pathology due to cytochrome c oxidase deficiency is revealed by a new zebrafish model. *The Journal of biological chemistry*, 282(48), pp.34839–49.

Baertling, F. et al., 2014. A guide to diagnosis and treatment of Leigh syndrome. *Journal of neurology, neurosurgery, and psychiatry*, 85, pp.257–65.

Balaban, R.S., Nemoto, S. & Finkel, T., 2005. Mitochondria, oxidants, and aging. *Cell*, 120(4), pp.483–95.

Battisti, C. et al., 2004. Cell response to oxidative stress induced apoptosis in patients with Leber's hereditary optic neuropathy. *Journal of neurology, neurosurgery, and psychiatry*, 75(12), pp.1731–6.

Bénit, P., Lebon, S. & Rustin, P., 2009. Respiratory-chain diseases related to complex III deficiency. *Biochimica et biophysica acta*, 1793(1), pp.181–5.

Bergmann, A. & Steller, H., 2010. Apoptosis, stem cells, and tissue regeneration. *Science signaling*, 3(145), p.re8.

Beroukhim, R. et al., 2010. The landscape of somatic copy-number alteration across human cancers. *Nature*, 463(7283), pp.899–905.

Beverly, L.J. et al., 2013. BAK activation is necessary and sufficient to drive ceramide synthase-dependent ceramide accumulation following inhibition of BCL2-like proteins. *The Biochemical journal*, 452(1), pp.111–9.

Billen, L.P. et al., 2008. Bcl-XL inhibits membrane permeabilization by competing with Bax. *PLoS biology*, 6, pp.1268–1280.

Biswas, G., Anandatheerthavarada, H.K. & Avadhani, N.G., 2005. Mechanism of mitochondrial stress-induced resistance to apoptosis in mitochondrial DNA-depleted C2C12 myocytes. *Cell death and differentiation*, 12(3), pp.266–78.

Boatright, K.M. et al., 2003. A unified model for apical caspase activation. *Molecular cell*, 11(2), pp.529–41.

Bourgeron, T. et al., 1995. Mutation of a nuclear succinate dehydrogenase gene results in mitochondrial respiratory chain deficiency. *Nature*, 11, pp.144–149.

Brandt, U. et al., 2003. Proton pumping by NADH:ubiquinone oxidoreductase. A redox driven conformational change mechanism? *FEBS Letters*, 545(1), pp.9–17.

Breuer, M.E. et al., 2013. The role of mitochondrial OXPHOS dysfunction in the development of neurologic diseases. *Neurobiology of disease*, 51, pp.27–34.

Brinkmann, K. & Kashkar, H., 2014. Targeting the mitochondrial apoptotic pathway: a preferred approach in hematologic malignancies? *Cell Death and Disease*, 5(3), p.e1098.

De Brito, O.M. & Scorrano, L., 2008. Mitofusin 2 tethers endoplasmic reticulum to mitochondria. *Nature*, 456(7222), pp.605–10.

Brunelle, J.K. et al., 2007. Loss of Mcl-1 protein and inhibition of electron transport chain together induce anoxic cell death. *Molecular and cellular biology*, 27(4), pp.1222–35.

Bruno, C. et al., 1999. A stop-codon mutation in the human mtDNA cytochrome c oxidase I gene disrupts the functional structure of complex IV. *American journal of human genetics*, 65(3), pp.611–20.

Carrozzo, R. et al., 2004. Maternally-inherited Leigh syndrome-related mutations bolster mitochondrial-mediated apoptosis. *Journal of neurochemistry*, 90(2), pp.490–501.

Chandra, D., Liu, J.-W. & Tang, D.G., 2002. Early mitochondrial activation and cytochrome c up-regulation during apoptosis. *The Journal of biological chemistry*, 277(52), pp.50842–54.

Chipuk, J.E. et al., 2012. Sphingolipid metabolism cooperates with BAK and BAX to promote the mitochondrial pathway of apoptosis. *Cell*, 148(5), pp.988–1000.

Choi, S.-Y. et al., 2007. Cardiolipin deficiency releases cytochrome c from the inner mitochondrial membrane and accelerates stimuli-elicited apoptosis. *Cell death and differentiation*, 14(3), pp.597–606.

Clayton, D.A. & Vinograd, J., 1967. Circular Dimer and Catenate Forms of Mitochondrial DNA in Human Leukaemic Leucocytes. *Nature*, 216, pp.652–657.

Coles, C.J. et al., 1979. Characterization of the iron-sulfur centers in succinate dehydrogenase. *Proceedings of the National Academy of Sciences of the United States of America*, 76(8), pp.3805–8.

Compton, S. et al., 2011. Mitochondrial dysfunction impairs tumor suppressor p53 expression/function. *The Journal of biological chemistry*, 286(23), pp.20297–312.

Csordás, G. et al., 2006. Structural and functional features and significance of the physical linkage between ER and mitochondria. *The Journal of cell biology*, 174(7), pp.915–21.

Cui, H., Kong, Y. & Zhang, H., 2012. Oxidative stress, mitochondrial dysfunction, and aging. *Journal of signal transduction*, 2012, p.646354.

Danielson, S.R. et al., 2002. Cells bearing mutations causing Leber's hereditary optic neuropathy are sensitized to Fas-Induced apoptosis. *The Journal of biological chemistry*, 277(8), pp.5810–5.

Dbaibo, G.S. et al., 1998. P53-Dependent Ceramide Response To Genotoxic Stress. *The Journal of clinical investigation*, 102(2), pp.329–39.

Dean, E., 2008. Apoptosis in Neurodegeneration : Programmed Cell Death and its Role in Alzheimer ' s and Huntington ' s Diseases. *Eukaryon*, 4(March), pp.42–47.

Debray, F.-G. et al., 2011. LRPPRC mutations cause a phenotypically distinct form of Leigh syndrome with cytochrome c oxidase deficiency. *Journal of medical genetics*, 48(3), pp.183–9.

Dewson, G. et al., 2008. To trigger apoptosis, Bak exposes its BH3 domain and homodimerizes via BH3:groove interactions. *Molecular cell*, 30(3), pp.369–80.

Diaz, F. et al., 2012. A defect in the mitochondrial complex III, but not complex IV, triggers early ROS-dependent damage in defined brain regions. *Human molecular genetics*, 21(23), pp.5066–77.

Diaz, F., 2010. Cytochrome c oxidase deficiency: patients and animal models. *Biochimica et biophysica acta*, 1802(1), pp.100–10.

Diaz, F. et al., 2006. Cytochrome c oxidase is required for the assembly/stability of respiratory complex I in mouse fibroblasts. *Molecular and cellular biology*, 26(13), pp.4872–81.

Diaz, F. et al., 2005. Mice lacking COX10 in skeletal muscle recapitulate the phenotype of progressive mitochondrial myopathies associated with cytochrome c oxidase deficiency. *Human molecular genetics*, 14(18), pp.2737–48.

Diaz, F. et al., 2008. Pathophysiology and fate of hepatocytes in a mouse model of mitochondrial hepatopathies. *Gut*, 57(2), pp.232–42.

Dickson, D.W., 2004. Apoptotic mechanisms in Alzheimer neurofibrillary degeneration : cause or effect ? *The Journal of Clinical Investigation*, 114(1), pp.23–27.

DiMauro, S. et al., 1983. Benign infantile mitochondrial myopathy due to reversible cytochrome c oxidase deficiency. *Annals of neurology*, 14(2), pp.226–34.

Dimauro, S. & Davidzon, G., 2005. Mitochondrial DNA and disease. *Annals of medicine*, 37(3), pp.222–32.

Domina, A.M. et al., 2004. MCL1 is phosphorylated in the PEST region and stabilized upon ERK activation in viable cells, and at additional sites with cytotoxic okadaic acid or taxol. *Oncogene*, 23(31), pp.5301–15.

Dumitru, C. & Gulbins, E., 2006. TRAIL activates acid sphingomyelinase via a redox mechanism and releases ceramide to trigger apoptosis. *Oncogene*, 41, pp.5612–25.

Edlich, F. et al., 2011. Bcl-x(L) retrotranslocates Bax from the mitochondria into the cytosol. *Cell*, 145(1), pp.104–16.

Efremov, R.G., Baradaran, R. & Sazanov, L. a, 2010. The architecture of respiratory complex I. *Nature*, 465(7297), pp.441–5.

Elliott, H.R. et al., 2008. Pathogenic Mitochondrial DNA Mutations Are Common in the General Population. , pp.254–260.

Ellis, H.M. & Horvitz, H.R., 1986. Genetic control of programmed cell death in the nematode C. elegans. *Cell*, 44(6), pp.817–29.

Evan, G. & Littlewood, T., 1998. A Matter of Life and Cell Death. *Science*, 281(5381), pp.1317–1322.

Formichi, P. et al., 2004. DNA end labelling (TUNEL) in a 3 year old girl with Leigh syndrome and prevalent cortical involvement. *Journal of Neurology, Neurosurgery & Psychiatry*, 75(6), pp.930–932.

Friedman, J.R. et al., 2011. ER tubules mark sites of mitochondrial division. *Science (New York, N.Y.)*, 334(6054), pp.358–62.

Ganesan, V. et al., 2010. Ceramide and activated Bax act synergistically to permeabilize the mitochondrial outer membrane. *Apoptosis : an international journal on programmed cell death*, 15(5), pp.553–62.

Gardai, S.J. et al., 2004. Phosphorylation of Bax Ser184 by Akt regulates its activity and apoptosis in neutrophils. *The Journal of biological chemistry*, 279(20), pp.21085–95.

Garwood, C.J. et al., 2011. Astrocytes are important mediators of Aβ-induced neurotoxicity and tau phosphorylation in primary culture. *Cell death & disease*, 2(6), p.e167.

Geromel, V. et al., 2001. Superoxide-induced massive apoptosis in cultured skin fibroblasts harboring the neurogenic ataxia retinitis pigmentosa (NARP) mutation in the ATPase-6 gene of the mitochondrial DNA. *Human molecular genetics*, 10(11), pp.1221–8.

Gervais, G. et al., 1999. Involvement of Caspases in Proteolytic Cleavage of Alzheimer ' s Amyloid- ß Precursor Protein and Amyloidogenic A ß Peptide Formation Franc. , 97, pp.395–406.

Ghelli, A. et al., 2003. Leber's hereditary optic neuropathy (LHON) pathogenic mutations induce mitochondrial-dependent apoptotic death in transmitochondrial cells incubated with galactose medium. *The Journal of biological chemistry*, 278(6), pp.4145–50.

Di Giovanni, S. et al., 2001. Apoptosis and ROS detoxification enzymes correlate with cytochrome c oxidase deficiency in mitochondrial encephalomyopathies. *Molecular and cellular neurosciences*, 17(4), pp.696–705.

Van Goethem, G. et al., 2001. Mutation of POLG is associated with progressive external ophthalmoplegia characterized by mtDNA deletions. *Nature genetics*, 28(3), pp.211–2.

Goldkorn, T. et al., 1998. H2O2 acts on cellular membranes to generate ceramide signaling and initiate apoptosis in tracheobronchial epithelial cells. *Journal of cell science*, 111 (Pt 2, pp.3209–20.

Gorgoglione, V. et al., 2010. Ceramide-induced activation of cytosolic NADH/cytochrome c electron transport pathway: An additional source of energy for apoptosis. *Archives of biochemistry and biophysics*, 504(2), pp.210–20.

Grimm, S., 2013. Respiratory chain complex II as general sensor for apoptosis. *Biochimica et biophysica acta*, 1827(5), pp.565–72.

Hanada, K. et al., 2007. CERT and intracellular trafficking of ceramide. *Biochimica et biophysica acta*, 1771(6), pp.644–53.

Hanahan, D. & Weinberg, R. a, 2011. Hallmarks of cancer: the next generation. *Cell*, 144(5), pp.646–74.

Hannun, Y. a & Obeid, L.M., 2008. Principles of bioactive lipid signalling: lessons from sphingolipids. *Nature reviews. Molecular cell biology*, 9(2), pp.139–50.

Harner, M. et al., 2011. The mitochondrial contact site complex, a determinant of mitochondrial architecture. *The EMBO journal*, 30(21), pp.4356–70.

Hatefi, Y., Haavik, A.G. & Griffiths, D.E., 1962. Studies on the Electron Transfer System: XLI. REDUCED COENZYME Q (QH2)-CYTOCHROME c REDUCTASE. *J.Biol.Chem*, 237, pp.1681–1685.

Hatefi, Y. & Stempel, K.E., 1969. Isolation and Enzymatic Properties of the Mitochondrial Reduced Diphosphopyridine Nucleotide Dehydrogenase. *J.Biol.Chem*, 244, pp.2350–2357.

Hoeferlin, L.A. et al., 2013. Folate stress induces apoptosis via p53-dependent de novo ceramide synthesis and up-regulation of ceramide synthase 6. *The Journal of biological chemistry*, 288(18), pp.12880–90.

Holt, I.J., Harding, A.E. & Morgan-Hughes, J.A., 1988. Depletions of muscle mitochondrial DNA in patients with mitochondrial myopathies. *Nature*, 331, pp.717–719.

Horvath, R. et al., 2009. Molecular basis of infantile reversible cytochrome c oxidase deficiency myopathy. *Brain : a journal of neurology*, 132(Pt 11), pp.3165–74.

Horvath, S.E. & Daum, G., 2013. Lipids of mitochondria. *Progress in lipid research*, 52(4), pp.590–614.

Hsu, Y. & Youle, R.J., 1998. Bax in Murine Thymus Is a Soluble Monomeric Protein That Displays Differential Detergent-induced Conformations. *J.Biol.Chem*, 273, pp.10777–10783.

Hunte, C., Zickermann, V. & Brandt, U., 2010. Functional modules and structural basis of conformational coupling in mitochondrial complex I. *Science*, 329(5990), pp.448–51.

Ito, T. et al., 1997. Bcl-2 Phosphorylation Required for Anti-apoptosis Function. *Journal of Biological Chemistry*, 272(18), pp.11671–11673.

Kagan, V.E. et al., 2005. Cytochrome c acts as a cardiolipin oxygenase required for release of proapoptotic factors. *Nature chemical biology*, 1(4), pp.223–32.

Kashkar, H. et al., 2005. Acid sphingomyelinase is indispensable for UV light-induced Bax conformational change at the mitochondrial membrane. *The Journal of biological chemistry*, 280(21), pp.20804–13.

Kaukonen, J. et al., 2000. Role of Adenine Nucleotide Translocator 1 in mtDNA Maintenance. *Science*, 289(5480), pp.782–785.

Kawatani, M. et al., 2003. Transmembrane domain of Bcl-2 is required for inhibition of ceramide synthesis, but not cytochrome c release in the pathway of inostamycin-induced apoptosis. *Experimental Cell Research*, 286(1), pp.57–66.

Kelly, G. & Strasser, A., 2011. *The essential role of evasion from cell death in cancer*,

Kerr, J.F.R., Wyllie, A.H. & Currie, A.R., 1972. APOPTOSIS : A BASIC BIOLOGICAL PHENOMENON WITH WIDE-.

Kim, H. et al., 2009. Stepwise activation of BAX and BAK by tBID, BIM, and PUMA initiates mitochondrial apoptosis. *Molecular cell*, 36(3), pp.487–99.

King, M.P. & Attardi, G., 1989. Human cells lacking mtDNA: repopulation with exogenous mitochondria by complementation. *Science (New York, N.Y.)*, 246(4929), pp.500–3.

Kischkel, F.C. et al., 1995. Cytotoxicity-dependent APO-1 (Fas/CD95)-associated proteins form a death-inducing signaling complex (DISC) with the receptor. *The EMBO journal*, 14(22), pp.5579–88.

Kitada, T. et al., 1998. Mutations in the parkin gene cause autosomal recessive juvenile parkinsonim. , 169(1993), pp.166–169.

Kraytsberg, Y. et al., 2006. Mitochondrial DNA deletions are abundant and cause functional impairment in aged human substantia nigra neurons. *Nature genetics*, 38(5), pp.518–20.

Kruse, S.E. et al., 2008. Mice with mitochondrial complex I deficiency develop a fatal encephalomyopathy. *Cell metabolism*, 7(4), pp.312–20.

Kujoth, G.C. et al., 2005. Mitochondrial DNA mutations, oxidative stress, and apoptosis in mammalian aging. *Science (New York, N.Y.)*, 309(5733), pp.481–4.

Kumar, S., 2007. Caspase function in programmed cell death. *Cell death and differentiation*, 14(1), pp.32–43.

Kuwana, T. et al., 2002. Bid, Bax, and lipids cooperate to form supramolecular openings in the outer mitochondrial membrane. *Cell*, 111(3), pp.331–42.

Kwong, J.Q. et al., 2007. The mitochondrial respiratory chain is a modulator of apoptosis. *The Journal of cell biology*, 179(6), pp.1163–77.

Laviad, E.L. et al., 2008. Characterization of ceramide synthase 2: tissue distribution, substrate specificity, and inhibition by sphingosine 1-phosphate. *The Journal of biological chemistry*, 283(9), pp.5677–84.

Lee, H. et al., 2011. Mitochondrial ceramide-rich macrodomains functionalize Bax upon irradiation. *PloS one*, 6(6), p.e19783.

Leigh, D., 1951. Subacute necrotizing encephalomyelopathy in an infant. *Journal of neurology, neurosurgery, and psychiatry*, 14(3), pp.216–21.

Lessene, G., Czabotar, P.E. & Colman, P.M., 2008. BCL-2 family antagonists for cancer therapy. *Nature reviews. Drug discovery*, 7(12), pp.989–1000.

Leung, K.H. & Hinkle, P.C., 1975. Reconstitution of ion transport and respiratory control in vesicles formed from reduced coenzyme Q-cytochrome c reductase and phospholipids. *The Journal of biological chemistry*, 250(21), pp.8467–71.

Lev, S., 2012. Nonvesicular lipid transfer from the endoplasmic reticulum. *Cold Spring Harbor perspectives in biology*, 4(10).

Li, P. et al., 1997. Cytochrome c and dATP-dependent formation of Apaf-1/caspase-9 complex initiates an apoptotic protease cascade. *Cell*, 91(4), pp.479–89.

Lin, M.T. et al., 2002. High aggregate burden of somatic mtDNA point mutations in aging and Alzheimer ' s disease brain. , 11(2), pp.133–146.

Lin, M.T. & Beal, M.F., 2006. Mitochondrial dysfunction and oxidative stress in neurodegenerative diseases. *Nature*, 443(7113), pp.787–95.

Lindsten, T. et al., 2000. The combined functions of proapoptotic Bcl-2 family members bak and bax are essential for normal development of multiple tissues. *Molecular cell*, 6(6), pp.1389–99.

Lithgow, T. et al., 1994. The Protein Component Endoplasmic Mitochondrial Product of the Oncogene of the Nuclear Envelope , the Membrane Is a. , 5(April).

Liu, J. et al., 2008. Role of Phospholipid Scramblase 3 in the Regulation of Tumor Necrosis Factor-alpha Induced Apoptosis. *Biochemistry*, 47, pp.4518–4529.

Liu, X. et al., 1996. Induction of apoptotic program in cell-free extracts: requirement for dATP and cytochrome c. *Cell*, 86(1), pp.147–57.

López-Montero, I. et al., 2005. Rapid transbilayer movement of ceramides in phospholipid vesicles and in human erythrocytes. *The Journal of biological chemistry*, 280(27), pp.25811–9.

Lovell, J.F. et al., 2008. Membrane binding by tBid initiates an ordered series of events culminating in membrane permeabilization by Bax. *Cell*, 135(6), pp.1074–84.

Lutter, M. et al., 2000. Cardiolipin provides specificity for targeting of tBid to mitochondria. *Nature cell biology*, 2(10), pp.754–61.

Majamaa, K. et al., 1998. Epidemiology of A3243G, the mutation for mitochondrial encephalomyopathy, lactic acidosis, and strokelike episodes: prevalence of the mutation in an adult population. *American journal of human genetics*, 63(2), pp.447–54.

Manfredi, G. et al., 1995. A NEW MUTATION ASSOCIATED WITH MELAS IS LOCATED IN A MITOCHONDRIAL DNA POLYPEPTIDE-CODING GENE. *Neuromusc. Disord.*, 5(5), pp.391–398.

Martinou, J.-C. & Youle, R.J., 2011. Mitochondria in apoptosis: Bcl-2 family members and mitochondrial dynamics. *Developmental cell*, 21(1), pp.92–101.

Matoba, S. et al., 2006. P53 Regulates Mitochondrial Respiration. *Science (New York, N.Y.)*, 312(5780), pp.1650–3.

Matsko, C.M. et al., 2001. Mitochondrial lipid alterations during Fas- and radiation-induced apoptosis. *Biochemical and biophysical research communications*, 287(5), pp.1112–20.

Mirabella, M. et al., 2000. Apoptosis in mitochondrial encephalomyopathies with mitochondrial DNA mutations: a potential pathogenic mechanism. *Brain : a journal of neurology*, 123 (Pt 1, pp.93–104.

Mitchell, P., 1961. Coupling of phosphorylation to electron and hyrogen transfer by a chemi-osmotic type of mechanism.

Mizutani, Y., Kihara, A. & Igarashi, Y., 2005. Mammalian Lass6 and its related family members regulate synthesis of specific ceramides. *The Biochemical journal*, 390(Pt 1), pp.263–71.

Mootha, V.K. et al., 2003. Identification of a gene causing human cytochrome c oxidase deficiency by integrative genomics. *Proceedings of the National Academy of Sciences of the United States of America*, 100(2), pp.605–10.

Moraes, C.T. et al., 1992. Molecular analysis of the muscle pathology associated with mitochondrial DNA deletions. *Nature genetics*, 1, pp.359–367.

Moraes, C.T. et al., 1991. mtDNA depletion with variable tissue expression: a novel genetic abnormality in mitochondrial diseases. *American journal of human genetics*, 48(3), pp.492–501.

Moungjaroen, J. et al., 2006. Reactive Oxygen Species Mediate Caspase Activation and Apoptosis Induced by Lipoic Acid in Human Lung Epithelial Cancer Cells through Bcl-2 Down-Regulation. , 319(3), pp.1062–1069.

Mullen, T.D., Hannun, Y. a & Obeid, L.M., 2012. Ceramide synthases at the centre of sphingolipid metabolism and biology. *The Biochemical journal*, 441(3), pp.789–802.

Nass, M.M. & Nass, S., 1963. Intramitochondrial Fibers With Dna Characteristics. I. Fixation and Electron Staining Reactions. *The Journal of cell biology*, 19, pp.593–611.

Nicholson, D.. & Thornberry, N.A., 1997. Caspases: killer proteases. , 0004(97).

Nishino, I., Spinazzola, A. & Hirano, M., 1999. Thymidine Phosphorylase Gene Mutations in MNGIE, a Human Mitochondrial Disorder. *Science*, 283(5402), pp.689–692.

Nonaka, I. et al., 1988. Acta Muscle pathology in cytochrome c oxidase deficiency *. *Acta Neuropathologica*, 77, pp.152–160.

Novgorodov, S. a et al., 2011. Developmentally regulated ceramide synthase 6 increases mitochondrial Ca2+ loading capacity and promotes apoptosis. *The Journal of biological chemistry*, 286(6), pp.4644–58.

Obeid, L.M. et al., 1993. Programmed cell death induced by ceramide. *Science (New York, N.Y.)*, 259(5102), pp.1769–71.

Ogawa, S. & Lee, T.M., 1984. The relation between the internal phosphorylation potential and the proton motive force in mitochondria during ATP synthesis and hydrolysis. *The Journal of biological chemistry*, 259(16), pp.10004–11.

Orrenius, S., Gogvadze, V. & Zhivotovsky, B., 2007. Mitochondrial oxidative stress: implications for cell death. *Annual review of pharmacology and toxicology*, 47, pp.143–83.

Panjarian, S. et al., 2008. De novo N-palmitoylsphingosine synthesis is the major biochemical mechanism of ceramide accumulation following p53 up-regulation. *Prostaglandins & other lipid mediators*, 86(1-4), pp.41–8.

Di Paola, M., Cocco, T. & Lorusso, M., 2000. Ceramide interaction with the respiratory chain of heart mitochondria. *Biochemistry*, 39(22), pp.6660–8.

Pavlakis, S.G. et al., 1984. Mitochondrial Myopathy, Encephalopathy, Lactic Acidosis , and Strokelike Episodes : A Distinctive Clinical Syndrome. *Annals of neurology*, 16(4), pp.481–488.

Perier, C. et al., 2005. Complex I deficiency primes Bax-dependent neuronal apoptosis through mitochondrial oxidative damage. *Proceedings of the National Academy of Sciences of the United States of America*, 102(52), pp.19126–31.

Pfeiffer, K. et al., 2003. Cardiolipin stabilizes respiratory chain supercomplexes. *The Journal of biological chemistry*, 278(52), pp.52873–80.

La Piana, G. et al., 2005. Porin and cytochrome oxidase containing contact sites involved in the oxidation of cytosolic NADH. *Archives of biochemistry and biophysics*, 436(1), pp.91–100.

Piruat, J.I. et al., 2004. The Mitochondrial SDHD Gene Is Required for Early Embryogenesis , and Its Partial Deficiency Results in Persistent Carotid Body Glomus Cell Activation with Full Responsiveness to Hypoxia The Mitochondrial SDHD Gene Is Required for Early Embryogenesis , an. *Molecular and cellular biology*.

Potting, C. et al., 2013. TRIAP1/PRELI complexes prevent apoptosis by mediating intramitochondrial transport of phosphatidic acid. *Cell metabolism*, 18(2), pp.287–95.

Quintana, A. et al., 2010. Complex I deficiency due to loss of Ndufs4 in the brain results in progressive encephalopathy resembling Leigh syndrome. *Proceedings of the National Academy of Sciences of the United States of America*, 107(24), pp.4–9.

Raturi, A. & Simmen, T., 2013. Where the endoplasmic reticulum and the mitochondrion tie the knot: the mitochondria-associated membrane (MAM). *Biochimica et biophysica acta*, 1833(1), pp.213–24.

Ravichandran, K.S. & Lorenz, U., 2007. Engulfment of apoptotic cells: signals for a good meal. *Nature reviews. Immunology*, 7(12), pp.964–74.

Reddien, P.W., Cameron, S. & Horvitz, H.R., 2001. Phagocytosis promotes programmed cell death in C. elegans. *Nature*, 412(6843), pp.198–202.

Renault, T.T. & Chipuk, J.E., 2014. Death upon a kiss: mitochondrial outer membrane composition and organelle communication govern sensitivity to BAK/BAX-dependent apoptosis. *Chemistry & biology*, 21(1), pp.114–23.

Riebeling, C. et al., 2003. Two mammalian longevity assurance gene (LAG1) family members, trh1 and trh4, regulate dihydroceramide synthesis using different fatty acyl-CoA donors. *The Journal of biological chemistry*, 278(44), pp.43452–9.

Rohn, T.T. et al., 2008. Lack of pathology in a triple transgenic mouse model of Alzheimer's disease after overexpression of the anti-apoptotic protein Bcl-2. *The Journal of neuroscience : the official journal of the Society for Neuroscience*, 28(12), pp.3051–9.

Rohn, T.T., 2010. The role of caspases in Alzheimer's disease; potential novel therapeutic opportunities. *Apoptosis : an international journal on programmed cell death*, 15(11), pp.1403–9.

Rossmanith, W. et al., 2008. Isolated cytochrome c oxidase deficiency as a cause of MELAS. *Journal of medical genetics*, 45(2), pp.117–21.

Ruvolo, P.P. et al., 1999. Ceramide induces Bcl2 dephosphorylation via a mechanism involving mitochondrial PP2A. *The Journal of biological chemistry*, 274(29), pp.20296–300.

Salo, M.K. et al., 1992. Reversible mitochondrial myopathy with cytochrome c oxidase deficiency. *Archives of disease in childhood*, 67(8), pp.1033–5.

Sawada, M. et al., 2000. Influence of Bax or Bcl-2 overexpression on the ceramide-dependent apoptotic pathway in glioma cells. *Oncogene*, 19, pp.3508–3520.

Schara, U. et al., 2011. Acute liver failure with subsequent cirrhosis as the primary manifestation of TRMU mutations. *Journal of inherited metabolic disease*, 34(1), pp.197–201.

Schellenberg, B. et al., 2013. Bax exists in a dynamic equilibrium between the cytosol and mitochondria to control apoptotic priming. *Molecular cell*, 49(5), pp.959–71.

Schon, E. a, DiMauro, S. & Hirano, M., 2012. Human mitochondrial DNA: roles of inherited and somatic mutations. *Nature reviews. Genetics*, 13(12), pp.878–90.

Sena, L. a & Chandel, N.S., 2012. Physiological roles of mitochondrial reactive oxygen species. *Molecular cell*, 48(2), pp.158–67.

Shamas-Din, A. et al., 2013. tBid undergoes multiple conformational changes at the membrane required for Bax activation. *The Journal of biological chemistry*, 288(30), pp.22111–27.

Siskind, L. et al., 2010. The BCL-2 protein BAK is required for long-chain ceramide generation during apoptosis. *The Journal of biological chemistry*, 285(16), pp.11818–26.

Siskind, L.J. & Colombini, M., 2000. The lipids C2- and C16-ceramide form large stable channels. Implications for apoptosis. *The Journal of biological chemistry*, 275(49), pp.38640–4.

Siskind, L.J., Kolesnick, R.N. & Colombini, M., 2002. Ceramide channels increase the permeability of the mitochondrial outer membrane to small proteins. *The Journal of biological chemistry*, 277(30), pp.26796–803.

Soper, W., Decker, L. & Pedersen, L., 1979. Mitochondrial ATPase complex. A dispersed, cytochrome-deficient, oligomycin-sensitive preparation from rat liver containing molecules with a tripartite structural arrangement. *J.Biol.Chem*, 254, pp.11170–11176.

Spelbrink, J.N. et al., 2001. Human mitochondrial DNA deletions associated with mutations in the gene encoding Twinkle, a phage T7 gene 4-like protein localized in mitochondria. *Nature genetics*, 28(3), pp.223–31.

Stiban, J., Caputo, L. & Colombini, M., 2008. Ceramide synthesis in the endoplasmic reticulum can permeabilize mitochondria to proapoptotic proteins. *Journal of lipid research*, 49(3), pp.625–34.

Stiban, J., Fistere, D. & Colombini, M., 2006. Dihydroceramide hinders ceramide channel formation: Implications on apoptosis. *Apoptosis : an international journal on programmed cell death*, 11(5), pp.773–80.

Sun, F. et al., 2005. Crystal structure of mitochondrial respiratory membrane protein complex II. *Cell*, 121(7), pp.1043–57.

Suzuki, M., Youle, R.J. & Tjandra, N., 2000. Structure of Bax: coregulation of dimer formation and intracellular localization. *Cell*, 103(4), pp.645–54.

Tait, S.W.G. & Green, D.R., 2010. Mitochondria and cell death: outer membrane permeabilization and beyond. *Nature reviews. Molecular cell biology*, 11(9), pp.621–32.

Tirodkar, T.S. & Voelkel-Johnson, C., 2012. Sphingolipids in apoptosis. *Experimental oncology*, 34(3), pp.231–42.

Trifunovic, A., Wredenberg, A. & Falkenberg, M., 2004. Premature ageing in mice expressing defective mitochondrial DNA polymerase. , 429(May), pp.417–423.

Tsukihara, T. et al., 1996. The Whole Structure of the 13-Subunit Oxidized Cytochrome c Oxidase at 2.8 A. *Science*, 272(31), pp.1136–1144.

Turrens, J.F., 2003. Mitochondrial formation of reactive oxygen species. *The Journal of physiology*, 552(Pt 2), pp.335–44.

Vafai, S.B. & Mootha, V.K., 2012. Mitochondrial disorders as windows into an ancient organelle.

Valente, E.M. et al., 2004. Hereditary Early-Onset Parkinson ' s Disease Caused by Mutations in PINK1. , 304(May), pp.1158–1160.

Vance, J.E., 1990. Phospholipid synthesis in a membrane fraction associated with mitochondria. *The Journal of biological chemistry*, 265, pp.7248–7256.

Vempati, U.D., Torraco, A. & Moraes, C.T., 2009. Mouse models of oxidative phosphorylation dysfunction and disease. *Methods*, 46(4), pp.241–247.

Venkataraman, K. et al., 2002. Upstream of growth and differentiation factor 1 (uog1), a mammalian homolog of the yeast longevity assurance gene 1 (LAG1), regulates N-stearoyl-sphinganine (C18-(dihydro)ceramide) synthesis in a fumonisin B1-independent manner in mammalian cells. *The Journal of biological chemistry*, 277(38), pp.35642–9.

Walker, T. et al., 2009. Sorafenib and Vorinostat Kill Colon Cancer Cells by CD95- Dependent and -Independent Mechanisms. *Molecular Pharmacology*, 76(2), pp.342–355.

Wallace, D.C. et al., 1988. Mitochondrial DNA Mutation Associated with Leber's Hereditary Optic Neuropathy. *Science*, 242, pp.1427–1430.

Wang, E. et al., 1991. Inhibition of Sphingolipid Biosynthesis. , 266(22), pp.14486–14490.

Wang, J. et al., 2001. Increased in vivo apoptosis in cells lacking mitochondrial DNA gene expression. *Proceedings of the National Academy of Sciences of the United States of America*, 98(7), pp.4038–43.

Wanka, C. et al., 2012. Synthesis of cytochrome C oxidase 2: a p53-dependent metabolic regulator that promotes respiratory function and protects glioma and colon cancer cells from hypoxia-induced cell death. *Oncogene*, 31(33), pp.3764–76.

Watt, I.N. et al., 2010. Bioenergetic cost of making an adenosine triphosphate molecule in animal mitochondria. *Proceedings of the National Academy of Sciences of the United States of America*, 107(39), pp.16823–7.

Westphal, D., Kluck, R.M. & Dewson, G., 2014. Building blocks of the apoptotic pore: how Bax and Bak are activated and oligomerize during apoptosis. *Cell death and differentiation*, 21(2), pp.196–205.

White-Gilbertson, S. et al., 2009. Ceramide synthase 6 modulates TRAIL sensitivity and nuclear translocation of active caspase-3 in colon cancer cells. *Oncogene*, 28(8), pp.1132–41.

Wiegmann, K. et al., 1994. Functional Dichotomy of Neutral and Acidic Sphingomyelinases in Tumor Necrosis Factor Signaling. *Cell*, 79, pp.1005–1015.

Wikström, M.K.F., 1977. Proton pump coupled to cytochrome c oxidase in mitochondria. *Nature*, 266, pp.271–273.

Williams, J.R., Little, J.. & Shipley, W.U., 1974. Association of mammalian cell death with specific endonucleolytic degradation of DNA.

Willis, S.N. et al., 2005. Proapoptotic Bak is sequestered by Mcl-1 and Bcl-xL, but not Bcl-2, until displaced by BH3-only proteins. *Genes & development*, 19(11), pp.1294–305.

Wood-Kaczmar, A. et al., 2008. PINK1 is necessary for long term survival and mitochondrial function in human dopaminergic neurons. *PloS one*, 3(6), p.e2455.

Wyllie, A.H., Kerr, J.F.R. & Currie, A.R., 1980. Cell death: the significance of apoptosis. *International review of cytology*, 68, pp.251–306.

Xia, D. et al., 1997. Crystal Structure of the Cytochrome bc1 Complex from Bovine Heart Mitochondria. *Science*, 277(5322), pp.60–66.

Ylikallio, E. & Suomalainen, A., 2012. Mechanisms of mitochondrial diseases. *Annals of medicine*, 44(1), pp.41–59.

Youle, R.J. & Strasser, A., 2008. The BCL-2 protein family: opposing activities that mediate cell death. *Nature reviews. Molecular cell biology*, 9(1), pp.47–59.

Yuan, J. et al., 1993. The C. elegans cell death gene ced-3 encodes a protein similar to mammalian interleukin-1 beta-converting enzyme. *Cell*, 75(4), pp.641–52.

Zeharia, A. et al., 2009. Acute infantile liver failure due to mutations in the TRMU gene. *American journal of human genetics*, 85(3), pp.401–7.

Zha, H. et al., 1996. Proapoptotic Protein Bax Heterodimerizes with Bcl-2 and Homodimerizes with Bax via a Novel Domain (BH3) Distinct from BH1 and BH2. *Journal of Biological Chemistry*, 271(13), pp.7440–7444.

Zhu, X. et al., 2009. Pathogenic mutations of nuclear genes associated with mitochondrial disorders Pathogenic Mutations of Nuclear Genes Encoding OXPHOS Complex Structural Subunits. *Acta Biochim Biophys Sin*, 41(3), pp.179–187.

Zigdon, H. et al., 2013. Ablation of ceramide synthase 2 causes chronic oxidative stress due to disruption of the mitochondrial respiratory chain. *The Journal of biological chemistry*, 288(7), pp.4947–56.

Appendix

Vector map

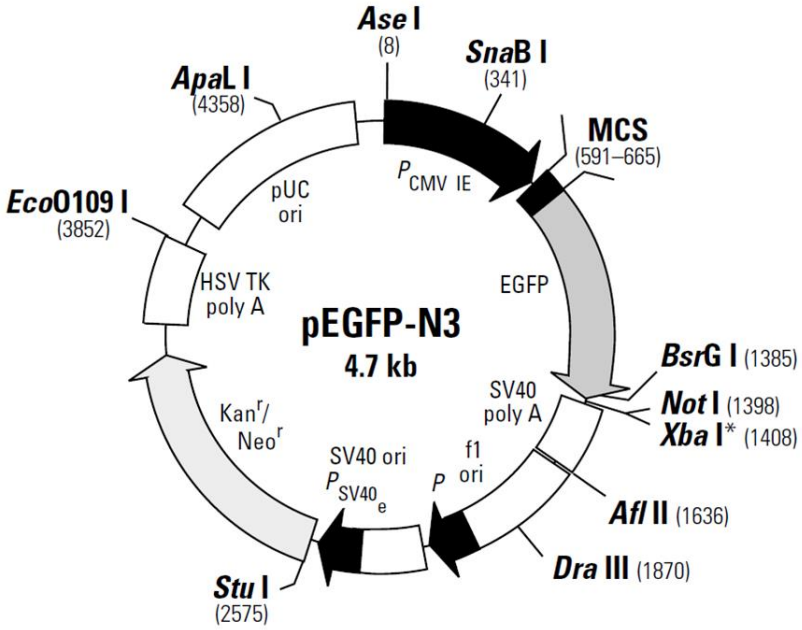

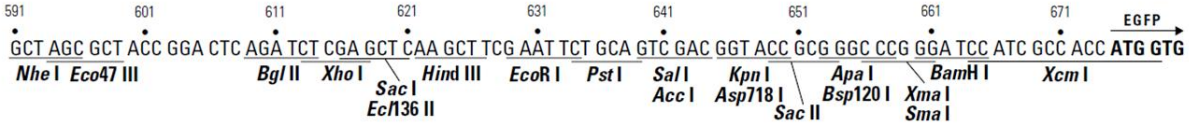

Erklärung

Ich versichere, dass ich die von mir vorgelegte Dissertation selbständig angefertigt, die benutzten Quellen und Hilfsmittel vollständig angegeben und die Stellen der Arbeit – einschließlich Tabellen, Karten und Abbildungen –, die anderen Werken im Wortlaut oder dem Sinn nach entnommen sind, in jedem Einzelfall als Entlehnung kenntlich gemacht habe; dass diese Dissertation noch keiner anderen Fakultät oder Universität zur Prüfung vorgelegen hat; dass sie noch nicht veröffentlicht worden ist sowie, dass ich eine solche Veröffentlichung vor Abschluss des Promotionsverfahrens nicht vornehmen werde. Die Bestimmungen dieser Promotionsordnung sind mir bekannt. Die von mir vorgelegte Dissertation ist von PD Dr. Hamid Kashkar, Prof. Dr. Elena Rugarli und Prof. Dr. Rudolf Wiesner betreut worden.